A METHOD FOR DETERMINING THE NUMBER OF DOMINANT MODES IN SINUSOIDAL STRUCTURAL RESPONSE

By

Ariel Franck

Thesis submitted to the Graduate Faculty of the
Virginia Polytechnic Institute and State University
in partial fulfillment of the requirements for the degree of
MASTER OF SCIENCE
in
Aerospace and Ocean Engineering

APPROVED:

Dr. W. L. Hallauer, Chairman

Dr. J. A. Weisshaar

Dr. F. H. Lutze, Jr.

May, 1978

Blacksburg, Virginia

ACKNOWLEDGEMENTS

The author wishes to express his gratitude to all the people who, in one way or another,helped him through his research. Special thanks are due to Dr. William L. Hallauer, his advisor, whose assistance , guidance and encouragement were invaluable, and to his wife, , for her patience and typing of the manuscript.

The author wishes to extend his gratitude to the Langley Research Center of the National Aeronautics and Space Administration for their financial support of this research through NASA Research Grant No. NSG 1276.

TABLE OF CONTENTS

LIST OF FIGURES

Figure Page

Figure Page

LIST OF TABLES

NOMENCLATURE

$[A]$	n x n complete transfer function matrix
$\underset{\sim}{A}_j$	The jth column of the transfer function matrix
$[A^*]$	p x k incomplete transfer function matrix
$\underset{\sim}{A}_j^*$	Incomplete jth column vector of $[A^*]$
$\|\|\underset{\sim}{A}_j^*\|\|$	The Hermitian length of the vector $\underset{\sim}{A}_j^*$
$[c]$	Damping matrix
$e_j^{(m)}$	The mth error corresponding to the jth vector
$E^{(i)}$	The ith total error
$\underset{\sim}{f}$	Column vector of exciting force
g_r	Damping value of the rth mode
$\underset{\sim}{h}_i$	p-dimensional complex orthogonal unit vector
$[H]$	p x p Hermitian matrix
$[k]$	Stiffness matrix
K_r	Constant dependent on frequency of excitation, generalized mass and damping of the rth mode
$[m]$	Mass matrix
M_r	Generalized mass of the rth mode
$\underset{\sim}{u}_i$	The ith eigenvector of $[H]$
$\underset{\sim}{x}$	Column vector of structural response
$\dot{\underset{\sim}{x}}$, $\ddot{\underset{\sim}{x}}$	Time derivatives of the response vector $\underset{\sim}{x}$
$\underset{\sim}{X}$	Complex response vector
$[Z]$	p x k incomplete transfer function matrix

$\underset{\sim}{Z}_j$	The jth complex vector of the incomplete transfer function matrix
$\|\|\underset{\sim}{Z}_j\|\|$	The Hermitian length of the vector $\underset{\sim}{Z}_j$
$\underset{\sim}{\phi}_r$	Mode shape of the rth mode
$\underset{\sim}{\phi}_r^*$	Incomplete mode shape of the rth mode
ϕ_{jr}	The jth element of the rth mode shape
ω	Frequency of excitation
ω_r	Natural frequency of the rth mode
λ_i	The ith eigenvalue of [H]

I. INTRODUCTION

The determination of the vibration characteristics of structures subject to dynamic loading is an important step in engineering design. One of the most common analytical tools to solve this problem is modal analysis, which is used to predict the dynamic response of structures.

In modal analysis of a given structure, the modes of vibration, that is the natural frequencies and the mode shapes, must be found first. Then, for arbitrary excitation, the spatial pattern of response of the structure at any instant is represented mathematically as a superposition of the mode shapes.

In experimental testing of structures, the quantities measured are precisely the natural frequencies and the mode shapes. This vibration testing is based on modal analysis, and it is often called modal testing. Theoretically, a continuous structure has an infinite number of modes of vibration. However, as Asher (1) observed, an extremely useful characteristic of structures is that only a small number of those modes are present when it is excited within a given frequency band. That is to say, the instantaneous spatial pattern of dynamic response to a given frequency band of excitation can be represented, with sufficient accuracy, as the superposition of the mode shapes corresponding to the relatively few modes active in that band. Modern techniques of modal testing

as described by Richardson (2), Miramand et al (3) and Hamma et al (4) make use of this characteristic. These methods use as input the transfer functions relating displacement (or acceleration) response to the forcing excitation generated at several points on the structure. These experimental data are then fit by a least-squares method or other curve-fitting procedure to equations based on modal analysis. These equations contain parameters such as natural frequencies and mode shapes. These modal parameters will be found from the solution of the curve-fitted equations.

As observed by Miramand et al (3), an essential quantity required in most curve-fitting algorithms is the number of modes to be included in the analytical model. This number is precisely the number of modes sensitive to excitation in a given frequency range, as discussed earlier. One classical way of finding that information is to plot one element of the transfer function (also called admittance) matrix versus frequency, and then to count the resonance peaks. This technique works well when the actual modes of the structure are widely separated in frequency or are very lightly damped. However, when several modes are grouped in a small frequency band or when structural damping is large, the number of modes cannot be accurately estimated by this method. It has been the objective of this research to develop a new and reliable method for determining

the number of dominant modes of a structure within a given frequency band.

The existence of two or more closely spaced modes is encountered often and usually presents a difficult problem in modal testing. It can happen that the modes are so close as to be indistinguishable even by the normally effective curve-fitting techniques. In this event, it is likely that an older method of modal testing known as Asher's method (1), also discussed by Hamma et al (4) and Hallauer and Stafford (5), would be tried. This method is essentially a multipoint excitation technique, which employs two or more shakers positioned in the structure in such a way as to separate the modes so that modal parameters can be measured directly.

Traill-Nash (6) also suggested that multipoint excitation techniques offered a means for exciting the pure undamped natural modes of a structure. He emphasized the importance of knowing the number of dominant modes (also referred to as "the number of effective degrees of freedom") of the structure for the frequency band of interest. Bishop and Gladwell (7) also discussed the advantage of knowing the number of dominant modes when the natural frequencies of a structure are to be determined. Asher (8) arrived at the same conclusion and he went further to propose a method for estimating the number of modes. However, numerical experiments with this method have shown it to be unreliable.

The number of active modes in the response in a given frequency region is an important and useful parameter. This parameter is helpful when trying to describe the response of the structure in that frequency region.

The method developed here to estimate this number of dominant modes uses as input only the admittance matrix (or some part of it). In general, this matrix would be obtained experimentally from the actual testing of a model. However, for the purposes of illustration, we have used numerically modelled structures to obtain the admittance matrices.

II. ANALYSIS

A. Mathematical Background

The concept of a "best approximating m-dimensional subspace" containing a set of vectors in a larger vector space was introduced and analyzed by Cliff (10) in the context of control theory. A concept analogous to that is the number of dominant modes of a vibrating structure. Given a set of p vectors in the space R^n, Cliff described a method for calculating an m-dimensional basis ($m < n$) which spans approximately, with an error minimized in the least squares sense, the set of p vectors. In other words, the p vectors are fit to the best approximating m-dimensional subspace. The following analysis employs this same general approach to find the number of dominant modes in the response of a structural system. Hence, the method developed is referred to as the vector fit method.

Consider a structural system with n discrete degrees of freedom represented mathematically as

$$[m]\ddot{\underset{\sim}{x}} + [c]\dot{\underset{\sim}{x}} + [k]\underset{\sim}{x} = \underset{\sim}{f}$$

where [m], [c] and [k] are the mass, damping and stiffness matrices, respectively. The vector $\underset{\sim}{x}$ denotes the column matrix of structural response and the vector $\underset{\sim}{f}$ denotes the column matrix of the forces. For steady-state sinusoidal forcing and response

at a frequency ω, we can write

$$\underset{\sim}{f} = \mathrm{Re}(\underset{\sim}{F}e^{i\omega t}) = \underset{\sim}{F}\cos\omega t$$

$$\underset{\sim}{x} = \mathrm{Re}(\underset{\sim}{X}e^{i\omega t})$$

where the complex response vector $\underset{\sim}{X}$ represents both amplitude and phase of response.

In general, using modal analysis with real or complex modes one can express the forced response in a series form,

$$\underset{\sim}{X} = \sum_{r=1}^{n} K_r(\omega)\underset{\sim}{\phi}_r\underset{\sim}{\phi}_r^t\underset{\sim}{F}$$

where $\underset{\sim}{\phi}_r$ is the mode shape corresponding to the rth mode, and $K_r(\omega)$ is a constant dependent on the generalized mass and damping of the rth mode. Then,the complete n x n tranfer function matrix is defined as

$$[A] = \sum_{r=1}^{n} K_r(\omega)\underset{\sim}{\phi}_r\underset{\sim}{\phi}_r^t$$

and any column of this matrix may be expressed as a linear sum of the n mode shape vectors,

$$\underset{\sim}{A}_j = \sum_{r=1}^{n} K_r(\omega)\phi_{jr}\underset{\sim}{\phi}_r$$

where ϕ_{jr} is the jth element of the column vector $\underset{\sim}{\phi}_r$.

A very common type of structural model described by modal analysis is a linearly elastic structure for which damping is assumed to be hysteretic and distributed spatially such that it

does not couple the undamped normal modes. For this type of model the mode shape vector of the rth mode, $\underset{\sim}{\phi}_r$, is real, and the constant $K_r(\omega)$ is complex. Only this type of model will be used for all numerical cases considered in this thesis. In this case, the constant K_r can be written

$$K_r(\omega) = \left\{ M_r \omega_r^2 \left[1 - \left(\frac{\omega}{\omega_r}\right)^2 + i g_r \right] \right\}^{-1}$$

where $$M_r = \underset{\sim}{\phi}_r^t \, [m] \, \underset{\sim}{\phi}_r$$

and ω_r, M_r and g_r are the natural frequency, generalized mass, and modal structural damping of the rth mode, respectively.

In the process of sinusoidal vibration testing, it is usually possible to measure the response at p stations on the structure, where almost invariably $p < n$. Thus, with a single shaker, say the jth, forcing at frequency ω, one can measure an incomplete column vector of the admittance matrix, which can be represented as

$$\underset{\sim}{A}_j^* = \sum_{r=1}^{n} K_r(\omega) \, \phi_{jr} \underset{\sim}{\phi}_r^*$$

where $\underset{\sim}{A}_j^*$ and $\underset{\sim}{\phi}_r^*$ are p-dimensional column vectors missing n - p elements from the corresponding vectors $\underset{\sim}{A}_j$ and $\underset{\sim}{\phi}_r$. Since the vectors $\underset{\sim}{\phi}_r^*$ are p-dimensional, at most only p of the n incomplete mode shape vectors are linearly independent. It seems reasonable

to expect that in general any subset of p $\underset{\sim}{\phi}_r^*$'s will, in fact, be independent.

We would expect that at any particular frequency of excitation, a subset q of the total modes dominates in the response. In this case, each $\underset{\sim}{A}_j^*$ should be a linear sum of the q $\underset{\sim}{\phi}_r^*$'s corresponding to the dominant modes. Then, the following procedure can be used to determine the number q:

A. If k shakers and p motion sensors are available, we measure the incomplete p x k transfer function matrix at frequency ω, whose columns are the $\underset{\sim}{A}_j^*$'s

$$\left[A^*\right] = \left[\underset{\sim}{A}_1^*, \underset{\sim}{A}_2^*, \ldots, \underset{\sim}{A}_k^*\right]$$

B. We can now analyze $\left[A^*\right]$ as follows:

(1) Determine a single p-dimensional unit vector $\underset{\sim}{h}_1$, unknown at this point, which can best approximate each column of the incomplete admittance matrix $\left[A^*\right]$ as a linear sum,

$$\underset{\sim}{A}_j^* = A_{j1}^{(1)} \underset{\sim}{h}_1 \quad , \quad j = 1, 2, \ldots, k$$

Calculate, in a sense to be defined, the error $E^{(1)}$ resulting from this representation.

(2) Determine two p-dimensional orthogonal unit vectors $\underset{\sim}{h}_1$

and $\underset{\sim}{h}_2$ which can best approximate each $\underset{\sim}{A}_j^*$ as a linear sum,

$$\underset{\sim}{A}_j^* = \sum_{i=1}^{2} A_{ji}^{(2)} \underset{\sim}{h}_i \quad , \quad j = 1, 2, \ldots, k$$

Calculate the error $E^{(2)}$ resulting from this representation.

.

.

.

(m) Determine the m p-dimensional unit vectors $\underset{\sim}{h}_1$, $\underset{\sim}{h}_2$, ... , $\underset{\sim}{h}_m$ which best represent each $\underset{\sim}{A}_j^*$ as a linear sum,

$$\underset{\sim}{A}_j^* = \sum_{i=1}^{m} A_{ji}^{(m)} \underset{\sim}{h}_i \quad , \quad j = 1, 2, \ldots, k$$

Calculate the error $E^{(m)}$ resulting from this representation.

If after q steps of this procedure we find $E^{(q)} << E^{(q-1)}$ and $E^{(q)} \simeq 0$, then we may reasonably conclude that each column vector $\underset{\sim}{A}_j^*$ is well represented by a sum of only q orthogonal vectors, and therefore, that there are q dominant modes in the response at that frequency of excitation. If $p < k$ and the procedure is carried through p steps, it is clear that $E^{(p)} = 0$, since the p inde-

pendent vectors $\underset{\sim}{h}_i$ span the subspace C^p. If, on the other hand, $k < p$ and the procedure is carried through k steps, then $E^{(k)} = 0$, since the k independent $\underset{\sim}{h}_i$ exactly span the subspace defined by the original k columns of the admittance matrix. Hence, in order for the proposed method to give a correct indication of the number of dominant modes, it is necessary that both p and k be greater than q. In other words, the number of sensors and the number of shakers each must exceed the number of dominant modes.

The theory required to carry out the calculations in step B above is developed next. To simplify the notation, we will denote the incomplete admittance matrix as

$$\left[A^*\right] = \left[Z\right] = \left[\underset{\sim}{Z}_1, \underset{\sim}{Z}_2, \ldots, \underset{\sim}{Z}_k\right]$$

Let a basis for C^p consist of p orthogonal unit vectors $\underset{\sim}{h}_1$, $\underset{\sim}{h}_2, \ldots, \underset{\sim}{h}_p$, which are unknown at this point. We can express any complex p-dimensional vector as the sum

$$\underset{\sim}{Z}_j = \left(\sum_{i=1}^{m} + \sum_{i=m+1}^{p} \right) \left(\bar{\underset{\sim}{h}}_i^t \underset{\sim}{Z}_j \right) \underset{\sim}{h}_i \quad , \quad j = 1, 2, \ldots, k$$

where $\bar{\underset{\sim}{h}}_i^t \underset{\sim}{Z}_j$ is a Hermitian scalar product as defined by Hildebrand (11). Since the unit vectors $\underset{\sim}{h}_i$ are orthogonal in the

Hermitian sense, then

$$||\underset{\sim}{Z}_j||^2 = \bar{\underset{\sim}{Z}}_j^t \underset{\sim}{Z}_j = \left(\sum_{i=1}^{m} + \sum_{i=m+1}^{p} \right) (\bar{\underset{\sim}{h}}_i^t \underset{\sim}{Z}_j)(\bar{\underset{\sim}{Z}}_j^t \underset{\sim}{h}_i)$$

Now, we may define as follows the squared error resulting from this representation of $\underset{\sim}{Z}_j$ as a series sum in only the first m of the $\underset{\sim}{h}_i$,

$$\left(e_j^{(m)}\right)^2 = \sum_{i=m+1}^{p} (\bar{\underset{\sim}{h}}_i^t \underset{\sim}{Z}_j)(\bar{\underset{\sim}{Z}}_j^t \underset{\sim}{h}_i)$$

$$= ||\underset{\sim}{Z}_j||^2 - \sum_{i=1}^{m} (\bar{\underset{\sim}{h}}_i^t \underset{\sim}{Z}_j)(\bar{\underset{\sim}{Z}}_j^t \underset{\sim}{h}_i)$$

It follows that an appropriate total error, in the least squares sense, for all the $\underset{\sim}{Z}_j$, j = 1, 2, ...,k, can be defined as

$$E^{(m)} = \left\{ \sum_{j=1}^{k} \left(e_j^{(m)}\right)^2 \right\}^{1/2}$$

$$= \left\{ \sum_{j=1}^{k} ||\underset{\sim}{Z}_j||^2 - \sum_{j=1}^{k} \sum_{i=1}^{m} (\bar{\underset{\sim}{h}}_i^t \underset{\sim}{Z}_j)(\bar{\underset{\sim}{Z}}_j^t \underset{\sim}{h}_i) \right\}^{1/2}$$

For a given m, we seek to minimize the error $E^{(m)}$, which corresponds to maximizing the double-summation term. Thus, we seek the $\underset{\sim}{h}_i$ so as to maximize that term, which can be rewritten in the more useful form,

$$\sum_{j=1}^{k} (\bar{h}_i^t \, Z_j)(\bar{Z}_j^t \, h_i) = \bar{h}_i^t \left(\sum_{j=1}^{k} Z_j \, \bar{Z}_j^t \right) h_i$$

$$= \bar{h}_i^t \, [Z][\bar{Z}]^t \, h_i$$

$$= \bar{h}_i^t \, [H] \, h_i$$

where $[H]$ is a p x p Hermitian matrix with p real positive eigenvalues $\lambda_1 \geq \lambda_2 \geq \ldots \geq \lambda_p$ and p corresponding complex, mutually orthogonal unit eigenvectors $u_1, u_2, \ldots, u_p$. Franklin (12) proves that the maximum value assumed by the Hermitian quadratic form $\bar{h}_1^t \, [H] \, h_1$ is the largest eigenvalue λ_1, and that the maximum results if we replace h_1 by u_1. Thus, we can write,

$$E_{min}^{(1)} = \left\{ \sum_{j=1}^{k} ||Z_j||^2 - \lambda_1 \right\}^{1/2}$$

Next we seek to minimize

$$E^{(2)} = \left\{ \sum_{j=1}^{k} ||Z_j||^2 - \lambda_1 - \bar{h}_2^t \, [H] \, h_2 \right\}^{1/2}$$

Franklin also proves that for all possible h_2 orthogonal to h_1, the maximum value assumed by the quadratic form $\bar{h}_2^t \, [H] \, h_2$ is the second eigenvalue λ_2, which results if $h_2 = u_2$. Thus,

$$E_{min}^{(2)} = \left\{ \sum_{j=1}^{k} ||Z_j||^2 - \sum_{i=1}^{2} \lambda_i \right\}^{1/2}$$

Following the same procedure, we can show that

$$E_{min}^{(m)} = \left\{ \sum_{j=1}^{k} ||\underset{\sim}{Z}_j||^2 - \sum_{i=1}^{m} \lambda_i \right\}^{\frac{1}{2}}$$

where $\underset{\sim}{h}_i = \underset{\sim}{u}_i$.

We can now reiterate and summarize the vector fit method for determining the number q of dominant modes at a given frequency.

(i) Using experimental or analytical data, assemble the p x k incomplete admittance matrix $[A^*]$ based upon k shaker locations and p sensor locations.

(ii) Form the p x p Hermitian matrix

$$[H] = [A^*][\bar{A}^*]^t$$

(iii) Calculate the eigenvalues of $[H]$, λ_i, i = 1, 2, ..., p. These eigenvalues will be real and positive.

(iv) For m = 1, 2, ..., p, calculate the minimized error

$$E_{min}^{(m)} = \left\{ \sum_{j=1}^{k} ||\underset{\sim}{A}_j^*||^2 - \sum_{i=1}^{m} \lambda_i \right\}^{\frac{1}{2}}$$

where $||\underset{\sim}{A}_j^*||$ is the Hermitian length of the jth column of $[A^*]$, $\underset{\sim}{A}_j^*$.

If there are in fact q dominant modes, then this would be indicated by the observation that $E^{(q)} << E^{(q-1)}$ and $E^{(q)} \simeq 0$. As

it will be seen later, in order for the analyst to judge the correct value of q, it is necessary that p and k each be greater than q.

B. Model Testing - Procedure

To demonstrate the validity of the vector fit method and to develop criteria for interpretation of the method, three different models were tested numerically. An interactive computer program in the Fortran language was developed to calculate and plot the errors $E^{(i)}$ from the modal parameters of the models. The analyst could vary the number and location of sensors and shakers, so as to simulate an incomplete admittance matrix. Appendix A contains the flow chart of the program.

Although the vector fit method has been developed for applications in experimental work, the admittance matrices in the following examples were generated numerically.

For ease of identification, the models tested will be referred to from now on as Model 1, Model 2 and Model 3. Their modal information, which includes the natural frequencies, generalized masses, hysteretic damping values and modal matrices, is shown in Tables 1, 2 and 3 respectively.

Model 1 is the five degree of freedom plane grid structure shown in Figure 1. This model, taken from Reference (9), has a pair of closely spaced modes, which is the motivation for including it

in the numerical evaluation.

In order to further test the method, models with greater numbers of dominant modes and more degrees of freedom were desirable. The limitation of the computer program to models having fewer than 25 degrees of freedom excluded the possibility of using more realistic discretized finite-element models having large numbers of degrees of freedom. It was necessary, therefore, to find models of suitably small size which, nevertheless, contained regions of high modal density.

To overcome this difficulty, it was decided to design the modal parameters of two other models directly, without attempting to represent any physical structural model. The modal parameters were selected to produce high modal density. The method used to design the models is described in Appendix B. It was thought appropriate to construct Model 2 with five degrees of freedom and with three dominant modes in order to study the behavior of the error in such a case, and to establish criteria for the interpretation of the larger model. The limited size of this model made it impossible to study the error curves for a considerably diminished admittance matrix.

Model 3 was constructed to have ten degrees of freedom so that much smaller incomplete admittance matrices could be tested, since the practical usefulness of the vector fit method certainly depends on its ability to detect the number of dominant modes

from such incomplete data. As a second feature added to this model, two separate regions of large modal activity were included, the first one with four dominant modes and the second with two dominant modes. This feature was added to see if the respective error curves would indeed behave independently, or if they would influence each other, causing a poor representation of the number of dominant modes.

To provide a reference condition, the error curves from the complete admittance matrix were calculated and plotted for each of the three models. Then, the errors from incomplete matrices were evaluated relative to this reference condition.

The tests on the models were run to check the following characteristics:

(1) The general behavior of the errors $E^{(i)}$;

(2) The error dependence upon shaker and sensor locations;

(3) The minimum size admittance matrix required to yield good results.

In actual experimental work one would generally expect to use more sensors than shakers on the model to be tested. This is so because shakers are usually large and difficult to position, whereas accelerometers are relatively small and can be attached to almost any exposed surface.

In order to illustrate better the dominant modes in a structure, Figure 2 and 3 were plotted. Figure 2 shows a plot versus frequency of the real and imaginary parts of the element corresponding to row 3 and column 3 of the admittance matrix of Model 1. Figure 3 shows the same type of plot for the element in row 4 and column 4 of Model 3. In Figure 2 the admittance element was plotted in the frequency range from 48.8 rad/sec to 57.8 rad/sec. In this region, the model has two closely spaced modes. The curves plotted represent both the exact admittance with all five modes included and the approximate admittance with only the two dominant modes included.

In Figure 3 the admittance element was plotted in the range from 45.0 rad/sec to 67.5 rad/sec, in which there are four dominant modes. The curves depict both the admittance element with all ten modes present and the same element with only the dominant modes present.

These figures illustrate two statements made before. First, it can be seen that only a few modes may approximate the structural response quite accurately; second, the number of dominant modes is not obvious from the number of peaks in these plots.

III. RESULTS AND DISCUSSION

The two closely spaced modes of Model 1 are at 53.501 and 55.409 rad/sec. This model was tested in the frequency range of 52.20 and 56.60 rad/sec. The complete admittance matrix was tested first, and the results are shown in Figure 4. According to the criterion established in Section II. A., we would conclude without doubt that there are two dominant modes in that range.

Next, the model was tested for four sensors and four shakers in various arrangements. Two of these cases are shown in Figures 5 and 6. The sensors and shakers excluded were selected arbitrarily. The qualitative interpretation of both Figures 5 and 6 is the same as that of Figure 4, namely, that two modes dominate the response. However, there are some quantitative differences that will be discussed later.

The Figures 7, 8 and 9 show the results of taking various combinations of only three shakers with five, four and three sensors respectively. In these examples, as well as in the previous two, the sensor locations differ somewhat from the shaker locations. Figures 7 and 8 show the errors resulting from non-square admittance matrices.

All these results agree qualitatively very well with our reference case of Figure 4, even when the small 3 x 3 admittance

matrix of Figure 9 was used.

To illustrate the quantitative differences, Figure 10 was plotted using the first errors $E^{(1)}$ of tests with decreasing admittance matrix sizes. The examples used correspond to the cases of Figures 4 (5 x 5 matrix), 5 (4 x 4 matrix) and 9 (3 x 3 matrix). The trend, which will also be seen for the other models, suggests that the absolute magnitude of the error depends on the size of the admittance matrix. However, the magnitude of the error does not convey any information, and the judgement on the number of dominant modes should arise from the relative sizes of the errors $E^{(1)}$, $E^{(2)}$,..., $E^{(m)}$ for a given admittance.

Testing of Model 2 yielded interesting results. This model has a region with three close dominant modes at 49.0, 51.0 and 55.0 rad/sec. It was tested in the frequency range from 48.2 to 54.5 rad/sec. Figure 11 shows the error curves for the complete admittance matrix, and its evaluation conclusively shows three dominant modes. Since the model has only five degrees of freedom, in order to have significant results for three dominant modes, at least a 4 x 4 admittance matrix was needed. It should be recalled that for k shakers, the kth error $E^{(k)}$ vanishes exactly. Figures 12, 13 and 14 show the results of such tests, the first two with 4 x 4 admittance matrices, and the last with a 5 x 4 admittance matrix. Evaluation of these cases leads to the same conclusion as the evaluation of the error

curves of Figure 11, namely, there are three dominant modes in this frequency band. Figure 13 is not as conclusive as the other figures, and it seems to indicate that two modes might suffice, but conservatism would favor the interpretation of three dominant modes.

As mentioned above, analysis of the larger Model 3 is very important. For this case, considerably diminished incomplete admittance matrices were considered. The first region of interest in Model 3 has four dominant modes at 49.0, 57.0, 59.0 and 65.0 rad/sec, and the second region has two dominant modes at 138.0 and 141.0 rad/sec. Figures 15 and 16 are the error curves for the complete admittance matrices for the two regions, respectively. Figure 16 clearly indicates two dominant modes, as expected. The interpretation of Figure 15, however, is not nearly so clear. If we relax the criterion that $E^{(q)} << E^{(q-1)}$ and consider rather the relative variations with frequency of $E^{(q-1)}$, $E^{(q)}$, $E^{(q+1)}$,..., then we will conclude from Figure 15 that three modes dominate in the 49 - 52 rad/sec and 60 - 64 rad/sec ranges, and that four modes dominate in the 52 - 60 rad/sec range. This seems to be a reasonable interpretation for Model 3. But this example indicates that a considerable amount of qualitative judgement may be required for correct interpretation of the vector fit method if there are several dominant modes.

For the first region of Model 3, Figures 17, 18 and 19 show

the results when the number of shakers was set to six, and the number of sensors was set to eight,seven and six, respectively. The results compare well with Figure 15. They all show a narrow frequency band with either three or four dominant modes. As stated earlier, it can be concluded that the general shapes of the error curves are quite similar and again, their magnitudes depend on the sizes of the admittance matrices.

Next, a set of tests were made for even smaller admittance matrices using only five shakers. Only Figure 20 is shown, since all the other results were quite similar. In this figure ten sensors were used, but the error curves could be interpreted as showing five dominant modes. It is clear, then, that the size of the admittance matrix, particularly the number of shakers used, is inadequate for this case, since the fifth error $E^{(5)}$ must vanish.

Finally, the model was tested in the region with two dominant modes. The results are shown in Figures 21, 22 and 23 for different shaker-sensor patterns. Figure 21 was obtained using six shakers and eight sensors, and the results agree with the reference case in Figure 16 showing two dominant modes. For the even smaller admittance matrices used in Figures 22 and 23, only three shakers and five sensors were used. These results also agree with our reference case and are most significant, since they show that a very small admittance matrix can be used. It can be seen that the indicated

number of dominant modes is independent of the locations of sensors and shakers. Again, even for the extreme cases of Figures 22 and 23, the vector fit method clearly gives the correct number of dominant modes.

It is evident that estimating the number of dominant modes from the error curves requires a somewhat qualitative judgement as to what constitutes a sufficiently small error. It is desirable, therefore, to infer from the numerical evaluations a "rule of thumb" criterion so as to check the validity of the estimate.

It has been seen that if there are q dominant modes and a sufficiently large admittance matrix with k shakers has been used ($k > q$), then the error $E^{(q)}$ is considerably smaller than $E^{(q-1)}$; furthermore, $E^{(q)}$, $E^{(q+1)}$, $E^{(q+2)}$,..., $E^{(k-1)}$ are nonzero but diminish progressively toward zero with very little variation with frequency; finally, $E^{(k)}$ is identically zero. This situation is best illustrated in Figures 4, 11 and 15. However, in cases where the admittance matrix is too small to permit observation of nonzero values of $E^{(q+1)}$, $E^{(q+2)}$, etc., we cannot be certain that the smallest nonzero error curve indicates the correct number of dominant modes. This type of a situation is illustrated in Figure 20. Hence, in order to provide an accurate estimate of the number of dominant modes, one should use an incomplete admittance matrix sufficiently large to produce at least one or two of the error curves $E^{(i)}$, where $i > q$.

IV. SUMMARY AND CONCLUSIONS

A vector fit method was developed to determine the number of dominant modes of a structure. It was tested on three numerically modeled structures. In all the tests, the choice of sensor and shaker locations was arbitrary..

The results in the first model were quite conclusive. The method did, in fact, detect the two dominant modes. In Model 2 the method also yielded good results, determining three dominant modes, although in one case the results were not as conclusive. In this case, the choice of sensor and shaker locations seemed inadequate. This suggests that, in the experimental setup, this choice should be made judiciously.

The size of Model 1 and 2 limited the possibilities of further study. Nevertheless, these two models illustrated the behavior of the error curves and helped establish the criteria by which the number of modes can be determined.

The most important results were obtained testing the vector fit method in Model 3. Due to the larger size of this model, it was possible to test cases with considerably diminished admittance matrices; hence the significance of these results. It was seen that for the region of high modal density (four dominant modes) the judgement as to the number of dominant modes required a closer inspection of the respective trends of the error curves.

In the region of two closely spaced modes of Model 3, the method detected the two modes quite well with an admittance matrix which was less than one half the complete matrix. This seems to indicate that the method could be very effective in actual experimental work.

In general, it can be concluded that the method is reliable provided that sufficiently large admittance matrices are employed.

It should be interesting to use actual experimental data as input to the vector fit method. Of particular interest is the method's sensitivity to experimental error in transfer function measurements.

REFERENCES

1. Asher, G.W., "A Method of Normal Mode Excitation Utilizing Admittance Measurements", Proceedings of the National Specialists Meeting on Dynamics and Aeroelasticity, Institute of Aerospace Sciences, Fort Worth, Texas, 1958.

2. Richardson, M., "Modal Analysis Using Digital Test Systems", Seminar on Understanding Digital Control and Analysis in Vibration Test Systems, a publication of The Shock and Vibration Information Center, May 1975.

3. Miramand, N., Billaud, J.F., Leleux, F. and Kervenez, J.P., "Identification of Structural Modal Parameters by Dynamic Tests at a single Point", The Shock and Vibration Bulletin, Bulletin 46, Part 5, 1976, pp. 197-212.

4. Hamma, G.A., Smith, S. and Stroud, R.C., "An Evaluation of Excitation and Analysis Methods for Modal Testing", SAE Paper No. 760872, Aerospace Engineering and Manufacturing Meeting, San Diego, 1976.

5. Hallauer, W.L. and Stafford J.F.,"On the Distribution of Shaker Forces in Multiple-shaker Modal Testing", submitted for publication, 1978.

6. Traill-Nash, R.W., "On the Excitation of Pure Natural Modes in Aircraft Resonance Testing", Journal of Aero/Space Sciences, December, 1958, pp. 775-778.

7. Bishop, R.E.D. and Gladwell,G.M.L., "An Investigation into the Theory of Resonance Testing", Philosophical Transactions of the Royal Society of London. Vol. 255, Series A, 1963.

8. Asher, G.M., "A Note on the Effective Degrees of Freedom of a Vibrating Structure", AIAA Journal, Volume 5, No. 4, 1966.

9. Shostak, A.G., "A Numerical Simulation of Modal Testing on a Structure with Viscous Damping", M.S. Thesis, Department of Aerospace and Ocean Engineering, VPI & SU, November 1977.

10. Cliff, E.M., "Essential Uncontrollability of Discrete, Linear, Time-Invariant, Dynamical Systems", Proceedings of IFAC 6th World Congress, Boston/Cambridge, Mass., August 1975.

11. Hildebrand, F.B., Methods of Applied Mathematics, 2nd Ed., Prentice-Hall, 1965.

12. Franklin, J.N., Matrix Theory, Prentice-Hall, New Jersey, 1968.

TABLES

TABLE 1

Modal Data of Model 1

Mode	Natural Frequency (rad/sec)	Generalized Mass M_r	Generalized Damping $M_r g_r \omega_r^2$
1	10.908	0.01229	0.04387
2	32.055	0.01123	0.34625
3	53.501	0.00932	0.80033
4	55.409	0.00862	0.79390
5	94.924	0.00680	1.83827

Modal Matrix

$\underset{\sim}{\phi}_1$	$\underset{\sim}{\phi}_2$	$\underset{\sim}{\phi}_3$	$\underset{\sim}{\phi}_4$	$\underset{\sim}{\phi}_5$
-0.12634	-0.94261	0.37951	-0.59473	-0.12141
-0.23221	-0.47940	0.07462	0.47750	0.71184
-0.33691	0.16540	0.70333	0.32015	-0.21661
-0.77298	-1.00000	-1.00000	1.00000	-1.00000
-1.00000	0.28130	-0.19504	-0.34187	0.13002

TABLE 2

Modal Data of Model 2

Mode	Natural Frequency (rad/sec)	Generalized Mass M_r	Generalized Damping $M_r g_r \omega_r^2$
1	20.00	0.0150	0.18
2	49.00	0.0100	0.96
3	51.00	0.0100	1.04
4	55.00	0.0034	1.03
5	80.00	0.0050	0.96

Modal Matrix

$\underset{\sim}{\phi}_1$	$\underset{\sim}{\phi}_2$	$\underset{\sim}{\phi}_3$	$\underset{\sim}{\phi}_4$	$\underset{\sim}{\phi}_5$
0.10	0.90	-0.30	-0.60	0.10
0.20	0.50	-0.10	0.50	-0.70
0.30	-0.20	-0.70	0.30	-0.20
0.80	1.00	1.00	1.00	1.00
1.00	-0.30	0.20	-0.30	-0.10

TABLE 3

Modal Data of Model 3

Mode	Natural Frequency (rad/sec)	Generalized Mass M_r	Generalized Damping $M_r g_r \omega_r^2$
1	12.00	0.0100	0.0432
2	25.00	0.0100	0.1875
3	49.00	0.0100	1.9120
4	57.00	0.0150	1.9494
5	59.00	0.0150	2.0890
6	65.00	0.0062	2.0881
7	95.00	0.0080	1.0821
8	138.00	0.0080	3.0520
9	141.00	0.0040	3.1800
10	205.00	0.0060	2.5210

Modal Matrix

$\underset{\sim}{\phi}_1$	$\underset{\sim}{\phi}_2$	$\underset{\sim}{\phi}_3$	$\underset{\sim}{\phi}_4$	$\underset{\sim}{\phi}_5$	$\underset{\sim}{\phi}_6$	$\underset{\sim}{\phi}_7$	$\underset{\sim}{\phi}_8$	$\underset{\sim}{\phi}_9$	$\underset{\sim}{\phi}_{10}$
0.15	-0.20	-0.30	-0.65	1.00	0.70	0.74	-0.53	0.40	0.60
1.00	1.00	0.10	0.20	0.30	0.05	-0.52	0.38	-0.55	-0.20
0.30	-0.45	0.71	0.30	0.62	1.00	-0.30	0.23	1.00	0.70
-0.50	0.50	1.00	0.50	-0.40	0.30	-0.80	0.71	0.60	-0.30
0.25	0.75	-0.15	0.53	0.81	-0.45	1.00	-0.42	0.01	0.65
-0.14	0.10	0.80	-0.28	-0.20	-0.55	0.24	0.51	0.30	1.00
0.80	-0.30	0.50	0.36	0.26	0.30	-0.68	1.00	-0.23	-0.40
0.05	-0.25	0.25	1.00	0.80	0.50	-0.13	-0.18	-0.80	0.55
-0.10	0.90	0.30	-0.70	-0.50	0.85	0.72	0.68	-0.20	0.15
0.70	0.12	0.60	0.15	-0.40	-0.15	0.66	-0.77	-0.30	0.68

FIGURES

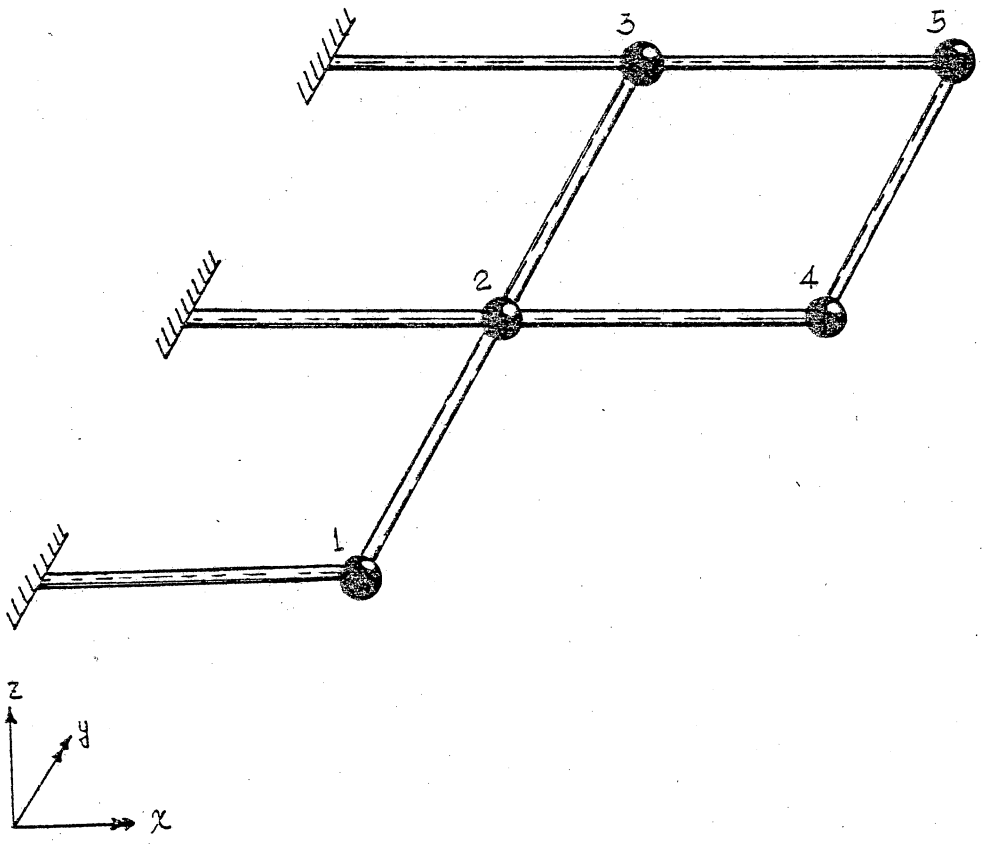

Beam Parameters:

Geometry: ¼ inch diameter, solid circular
Length: 10 inches
Bending Stiffness (EI): 1.917×10^3 lb-in^2
Torsional Stiffness (GJ): 1.534×10^3 lb-in^2

Figure 1 - Model 1, Cantilevered Plane Grid Structure

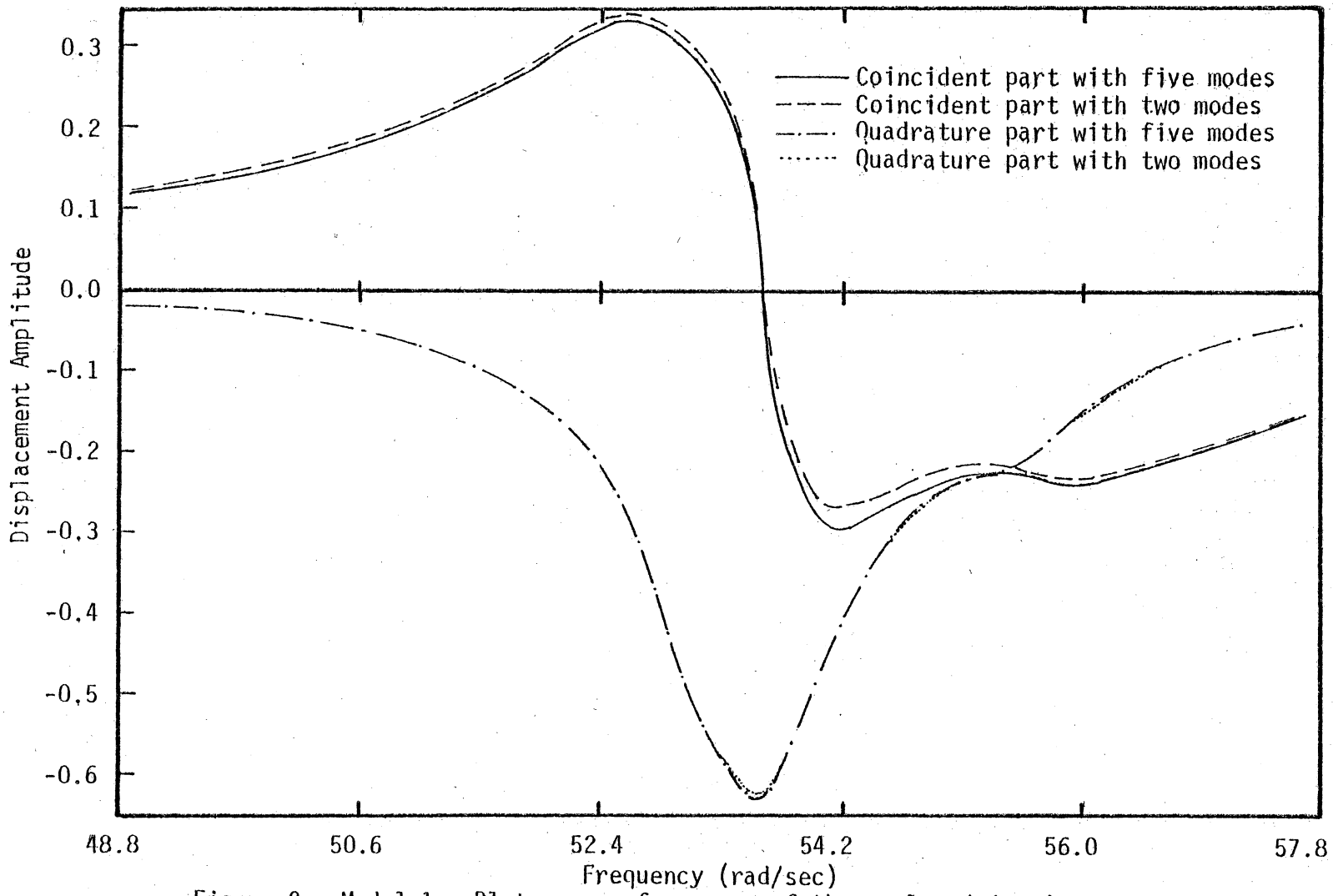

Figure 2.- Model 1 - Plot versus frequency of the real and imaginary parts of the element (3,3) of the admittance matrix with five and two modes.

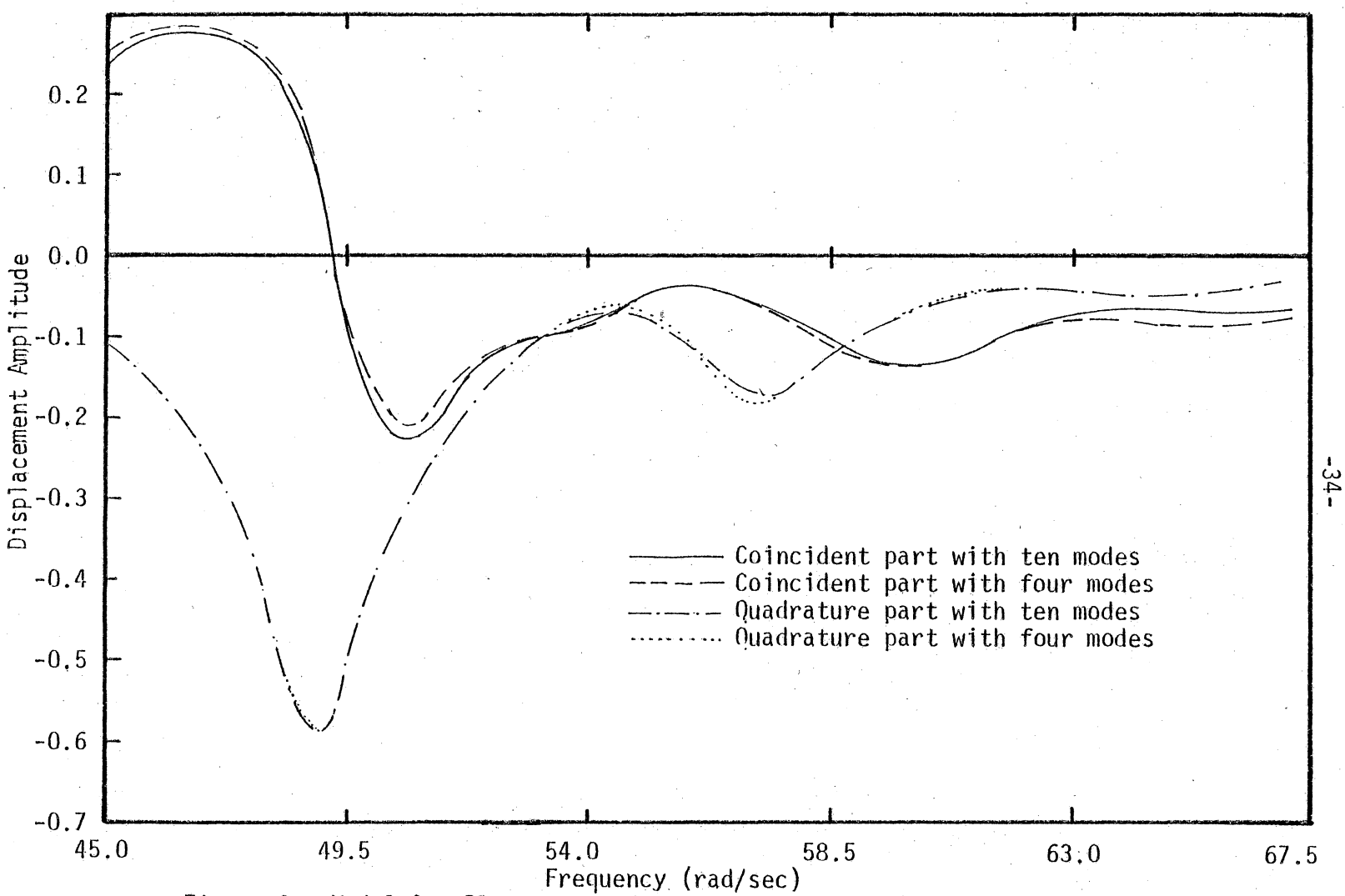

Figure 3.- Model 3 - Plot versus frequency of the real and the imaginary parts of the element (4,4) of the admittance matrix with ten and four modes.

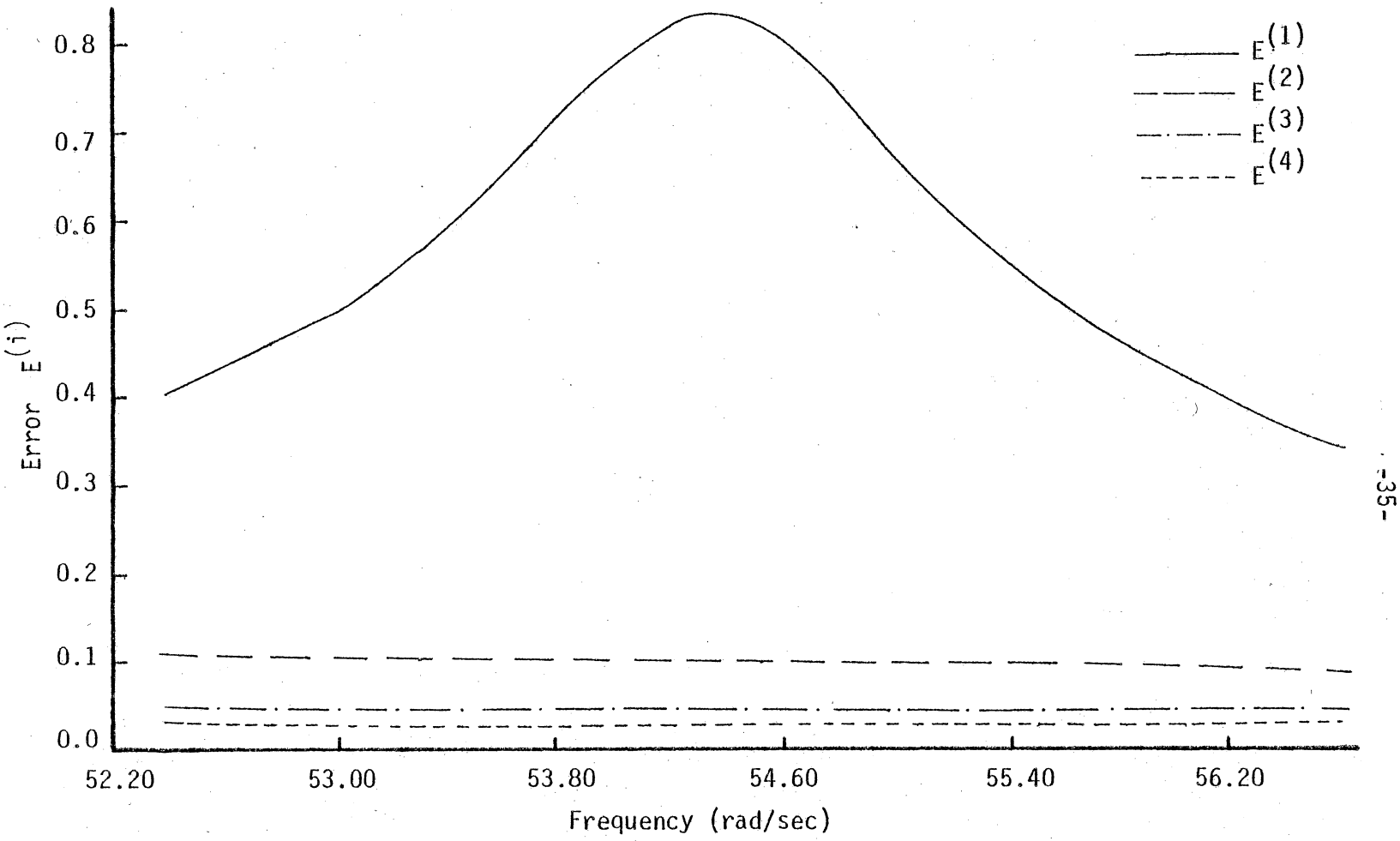

Figure 4.- Model 1 - Error plot with complete admittance matrix.

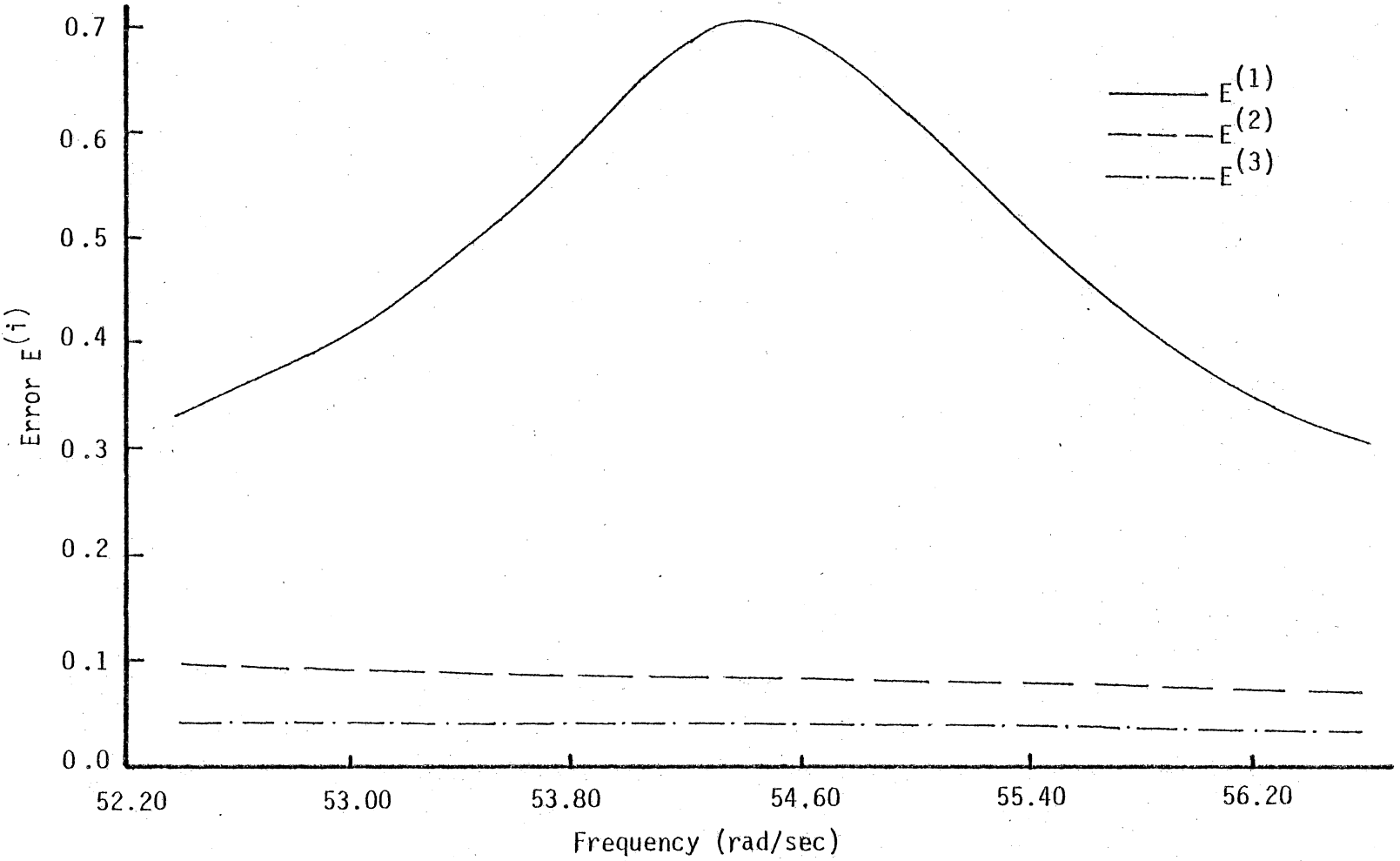

Figure 5.- Model 1 - Error plot with 4 sensors and 4 shakers.
Sensors located at dofs 1, 3, 4 and 5,
shakers located at dofs 1, 3, 4 and 5.

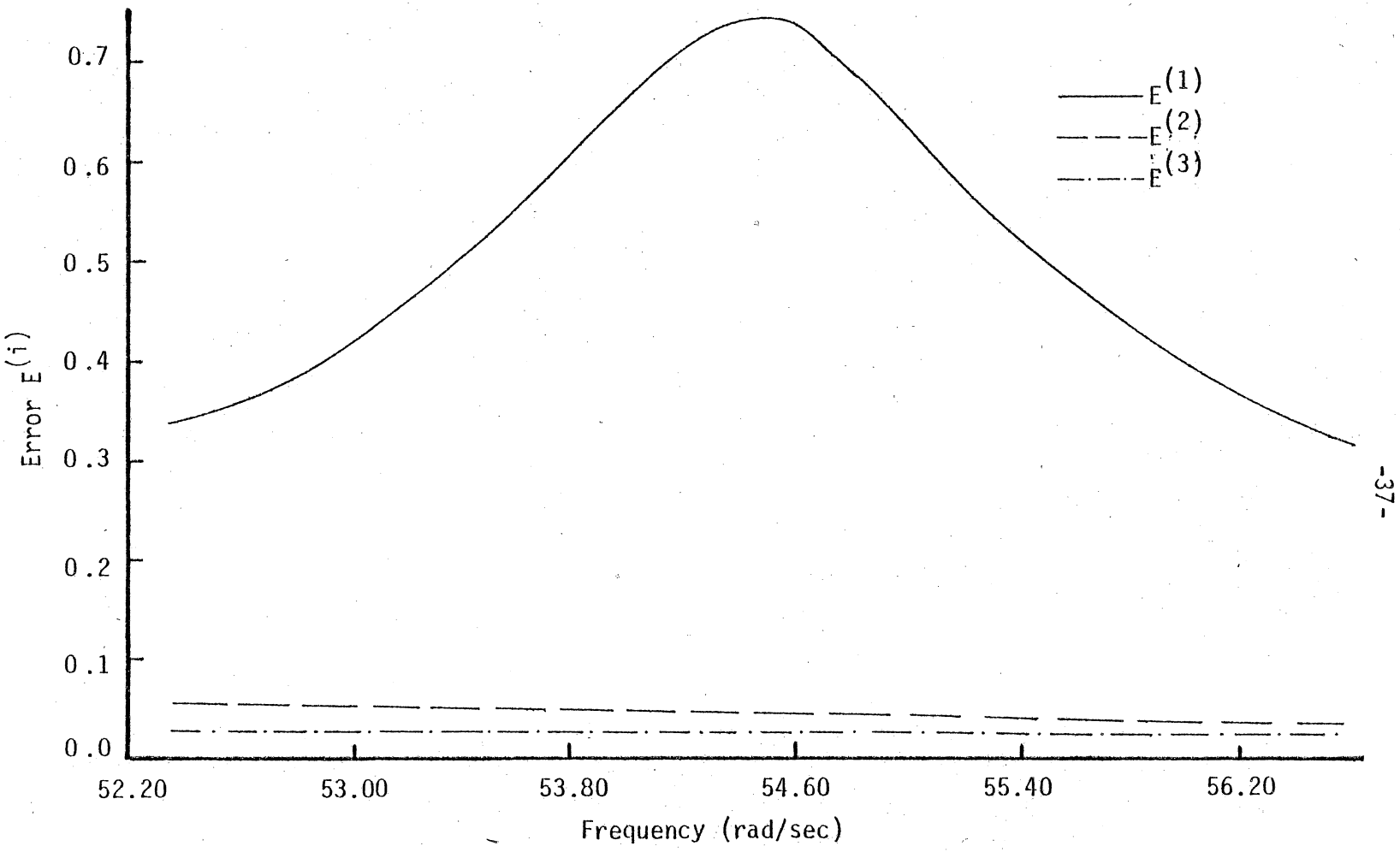

Figure 6.- Model 1 -Error plot with 4 sensors and 4 shakers.
Sensors located at dofs 2, 3, 4 and 5,
shakers located at dofs 1, 3, 4 and 5.

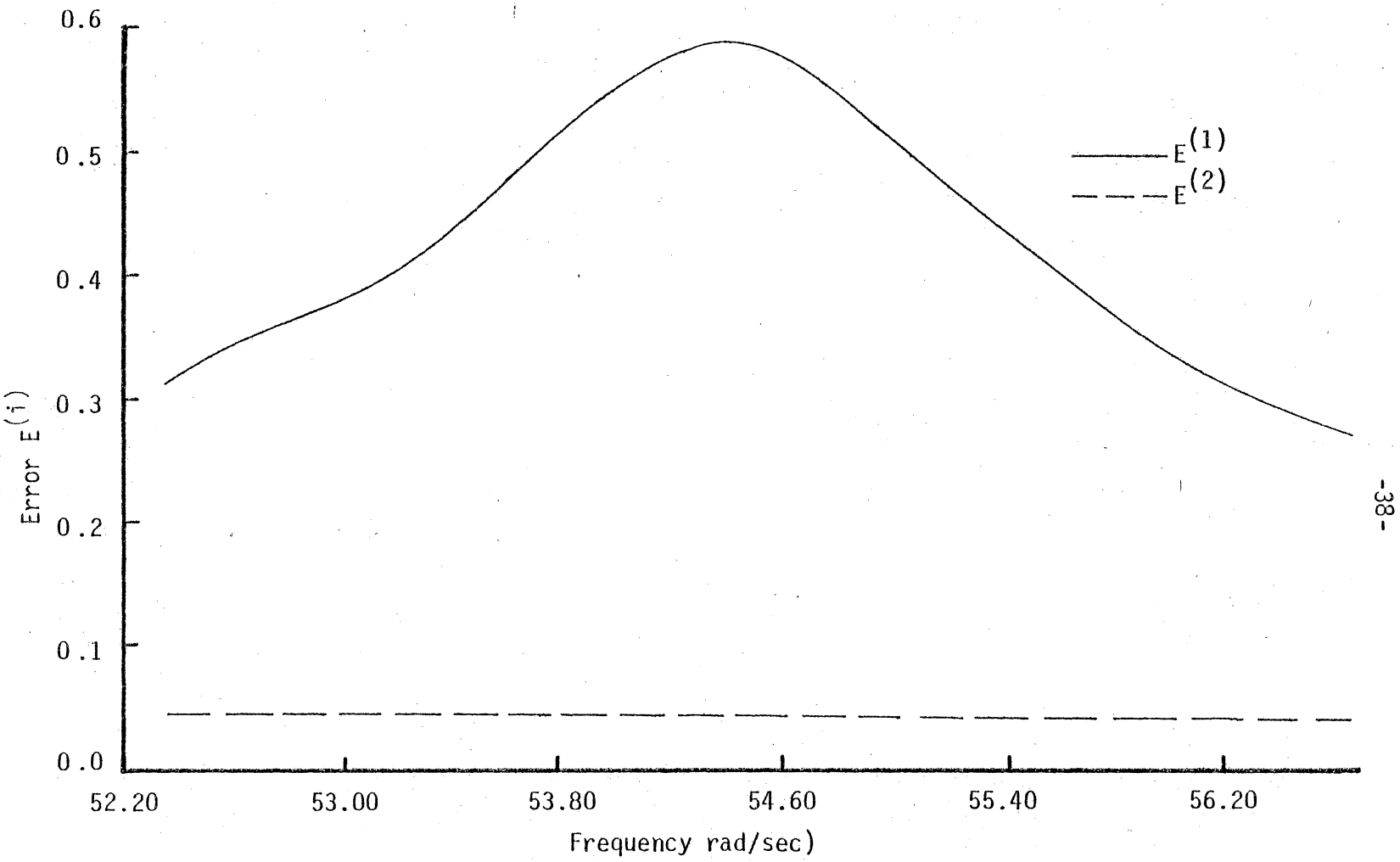

Figure 7.- Model 1 - Error plot with 5 sensors and 3 shakers. Sensors located at dofs 1, 2, 3, 4 and 5, shakers located at dofs 1, 3 and 5.

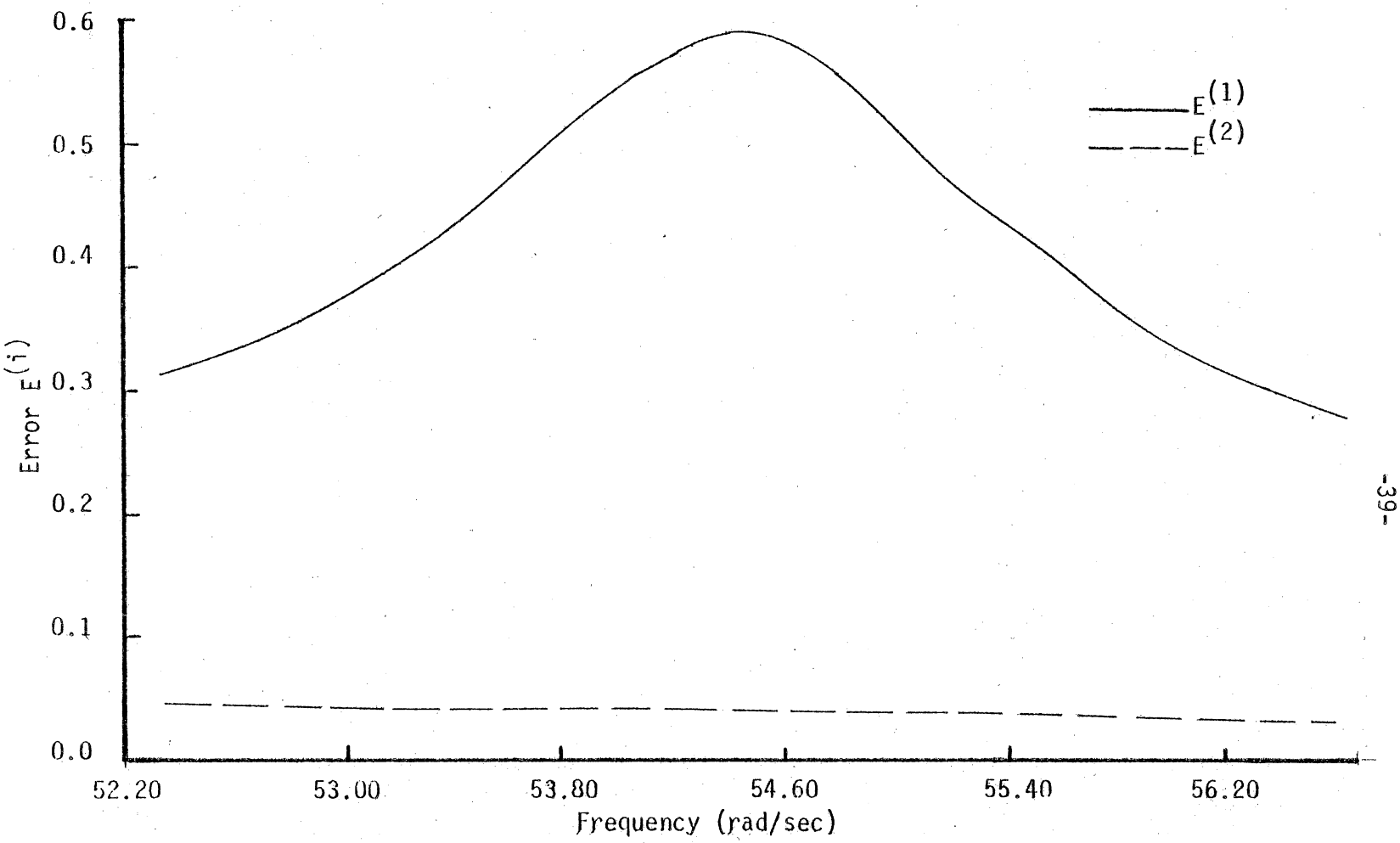

Figure 8.- Model 1 - Error plot with 4 sensors and 3 shakers. Sensors located at dofs 2, 3, 4 and 5, shakers located at dofs 1, 3 and 5.

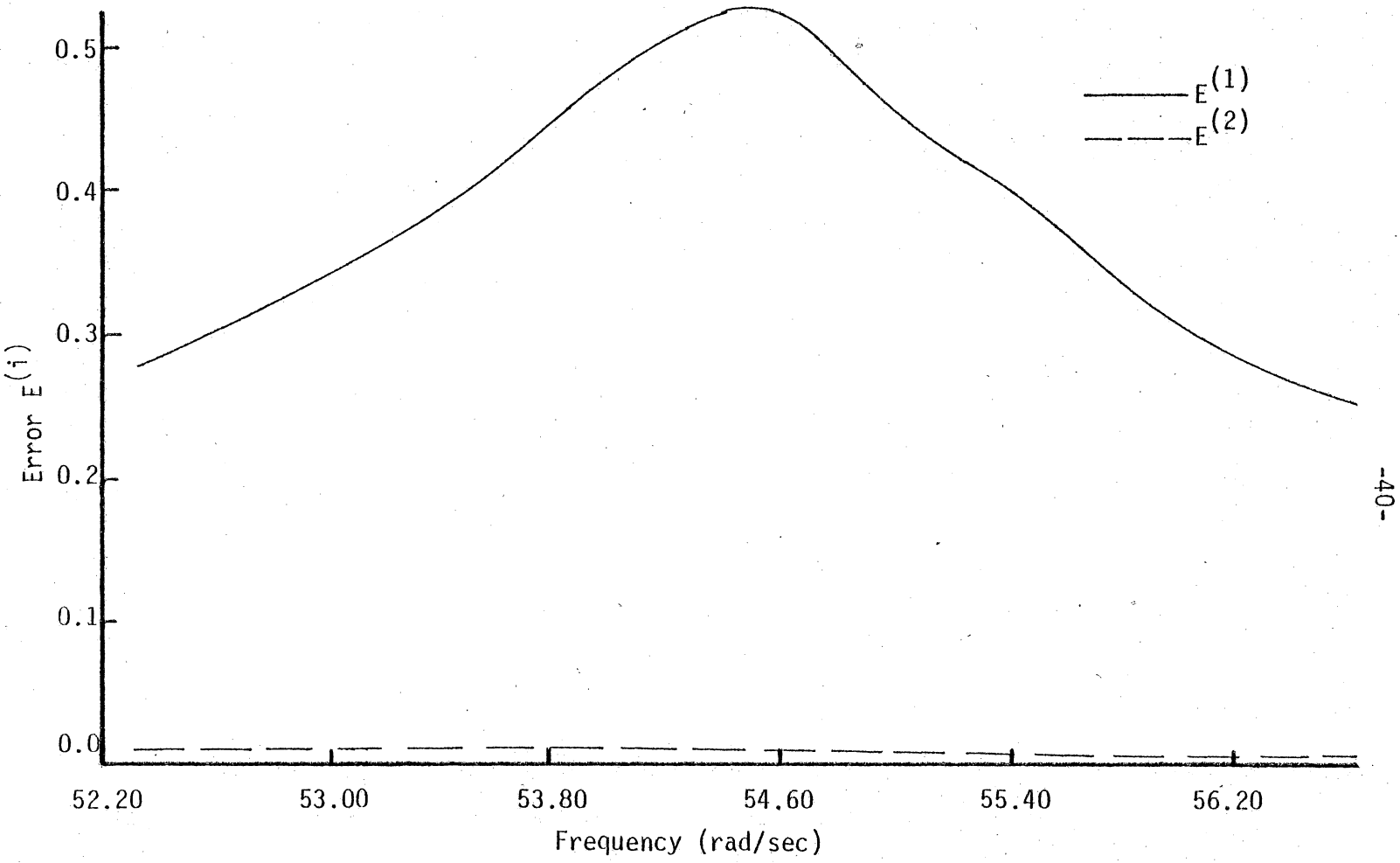

Figure 9.- Model 1 - Error plot with 3 sensors and 3 shakers; sensors located at dofs 1, 3 and 5, shakers located at dofs 2, 3 and 4.

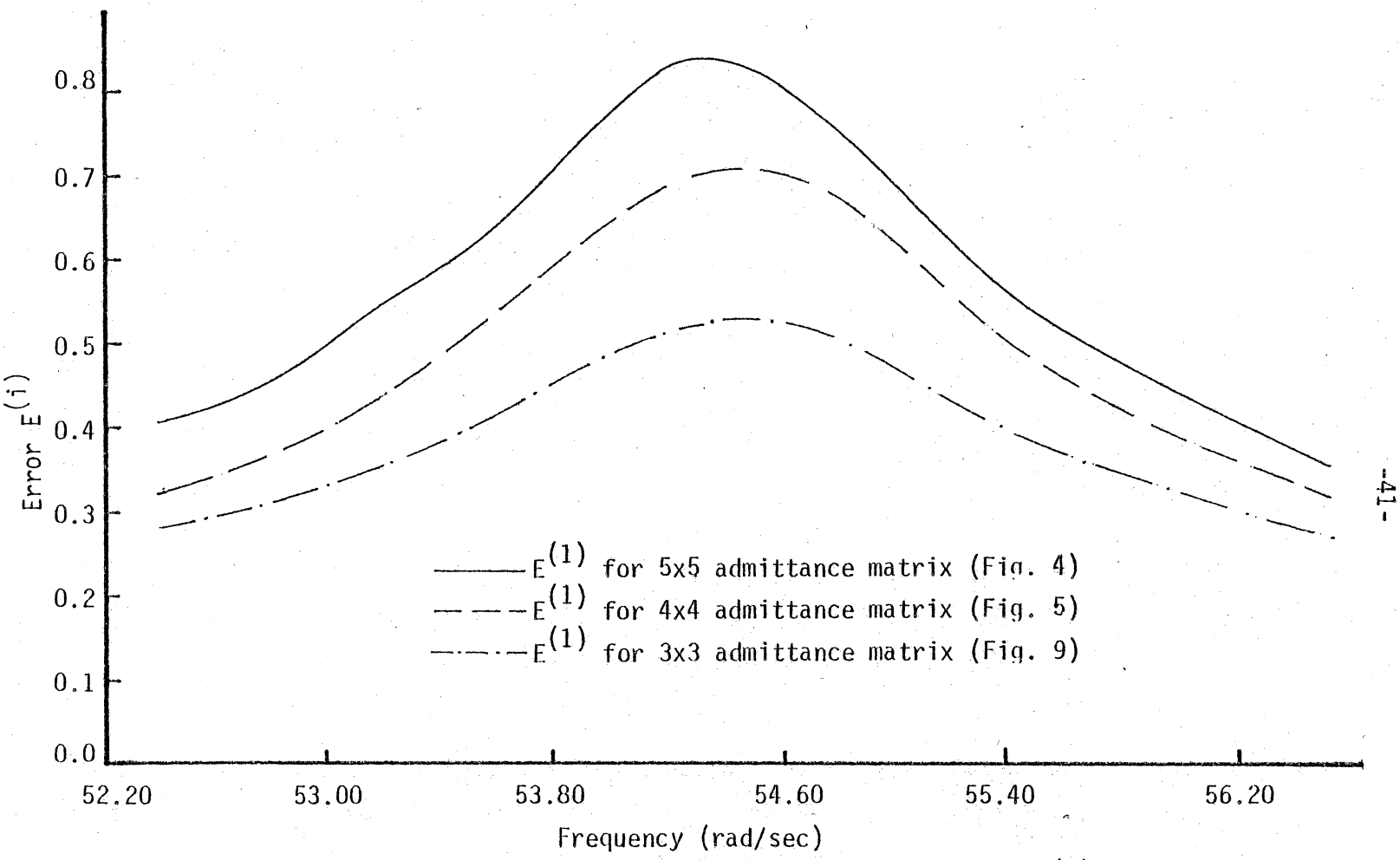

Figure 10.- Model 1 - Plot of the first error curves $E^{(1)}$ for cases in Figures 4, 5 and 9.

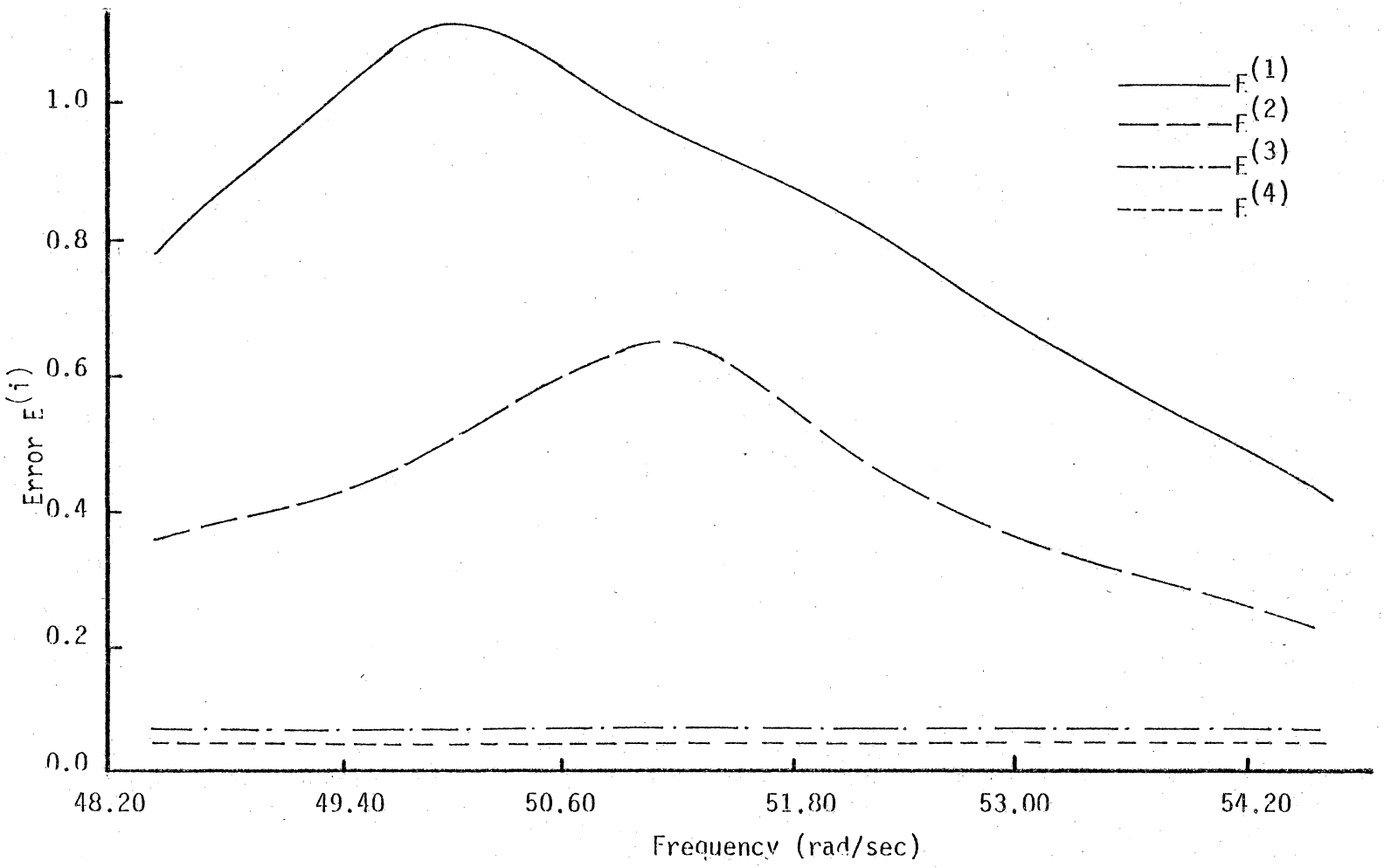

Figure 11.- Model 2 - Error plot with the complete admittance matrix.

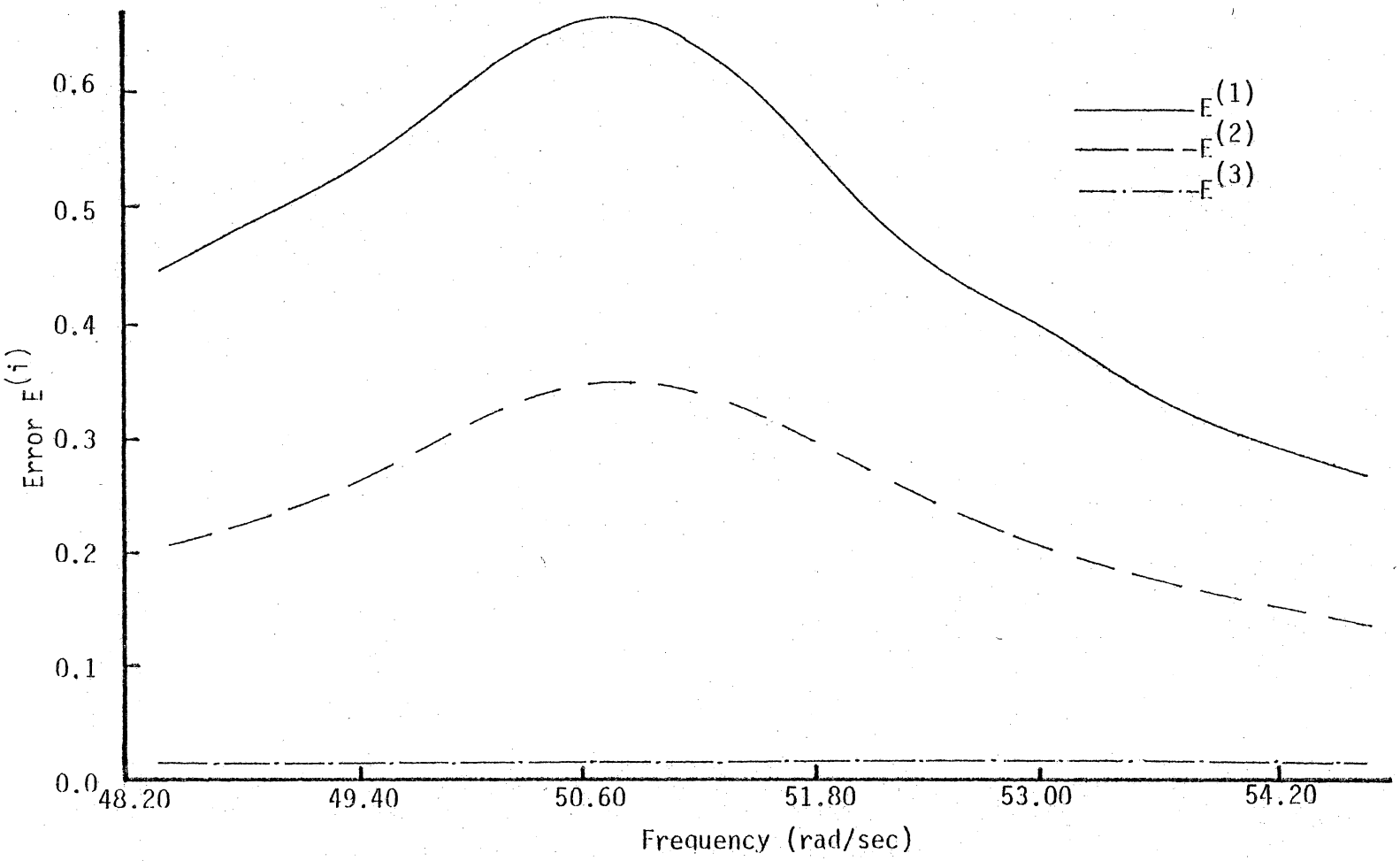

Figure 12.- Model 2 - Error plot with 4 sensors and 4 shakers. Sensors located at dofs 1, 2, 4 and 5, shakers located at dofs 1, 2, 3 and 5.

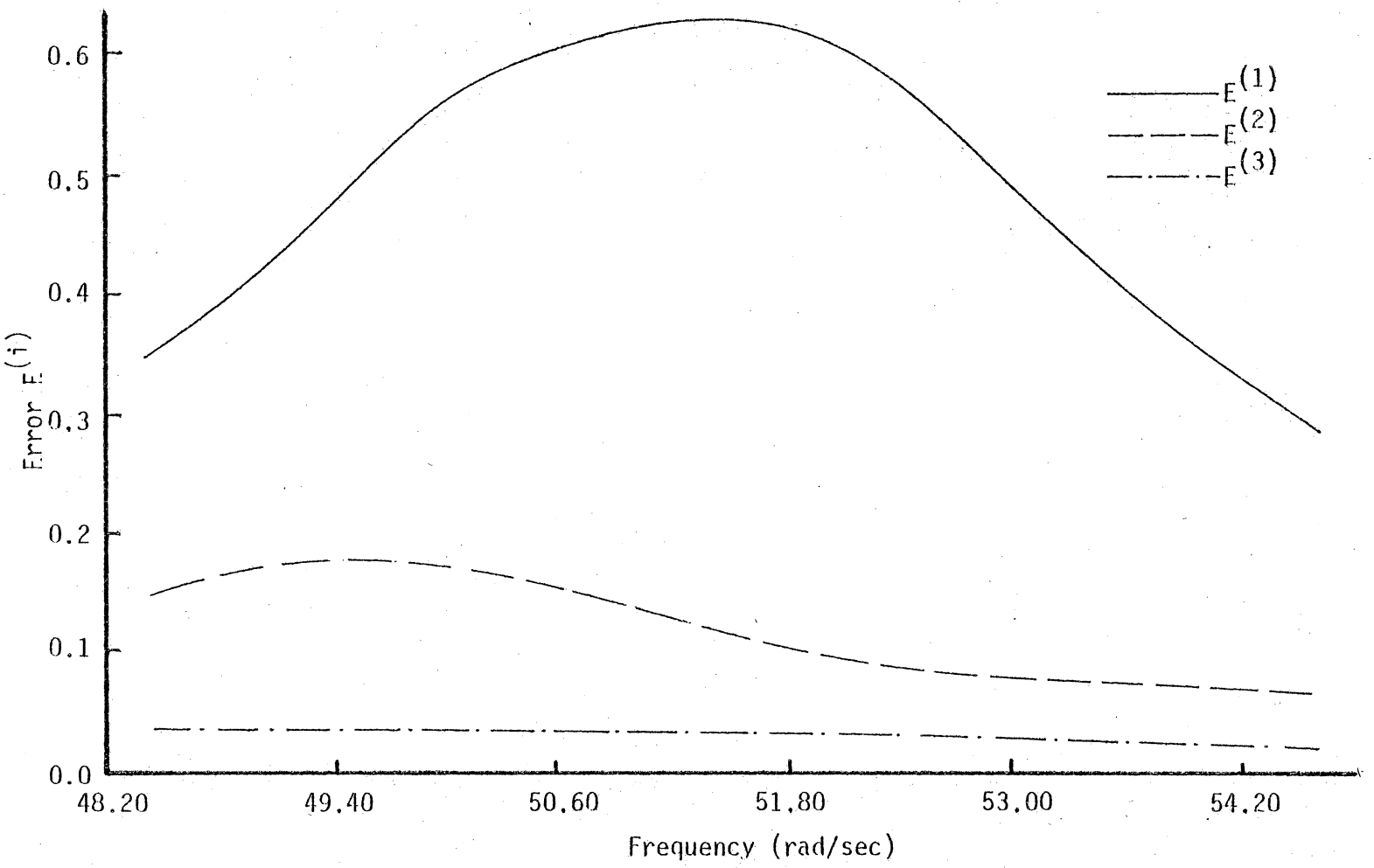

Figure 13.- Model 2 -Error plot with 4 sensors and 4 shakers
Sensors located at dofs 2, 3, 4 and 5,
shakers located at dofs 1, 2, 3 and 4.

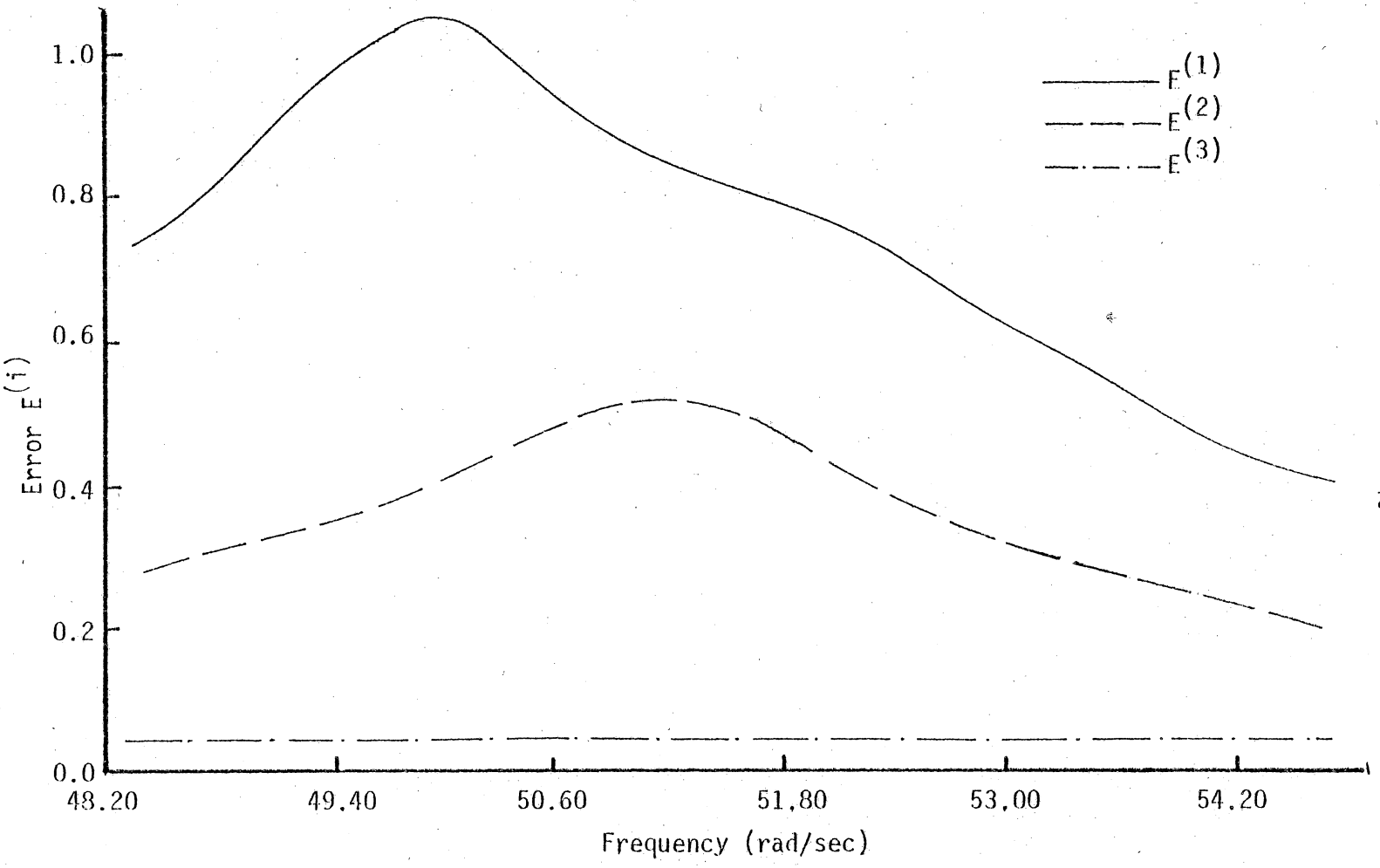

Figure 14.- Model 2 - Error plot with 5 sensors and 4 shakers
Sensors located at dofs 1, 2, 3, 4 and 5,
shakers located at dofs 1, 3, 4 and 5.

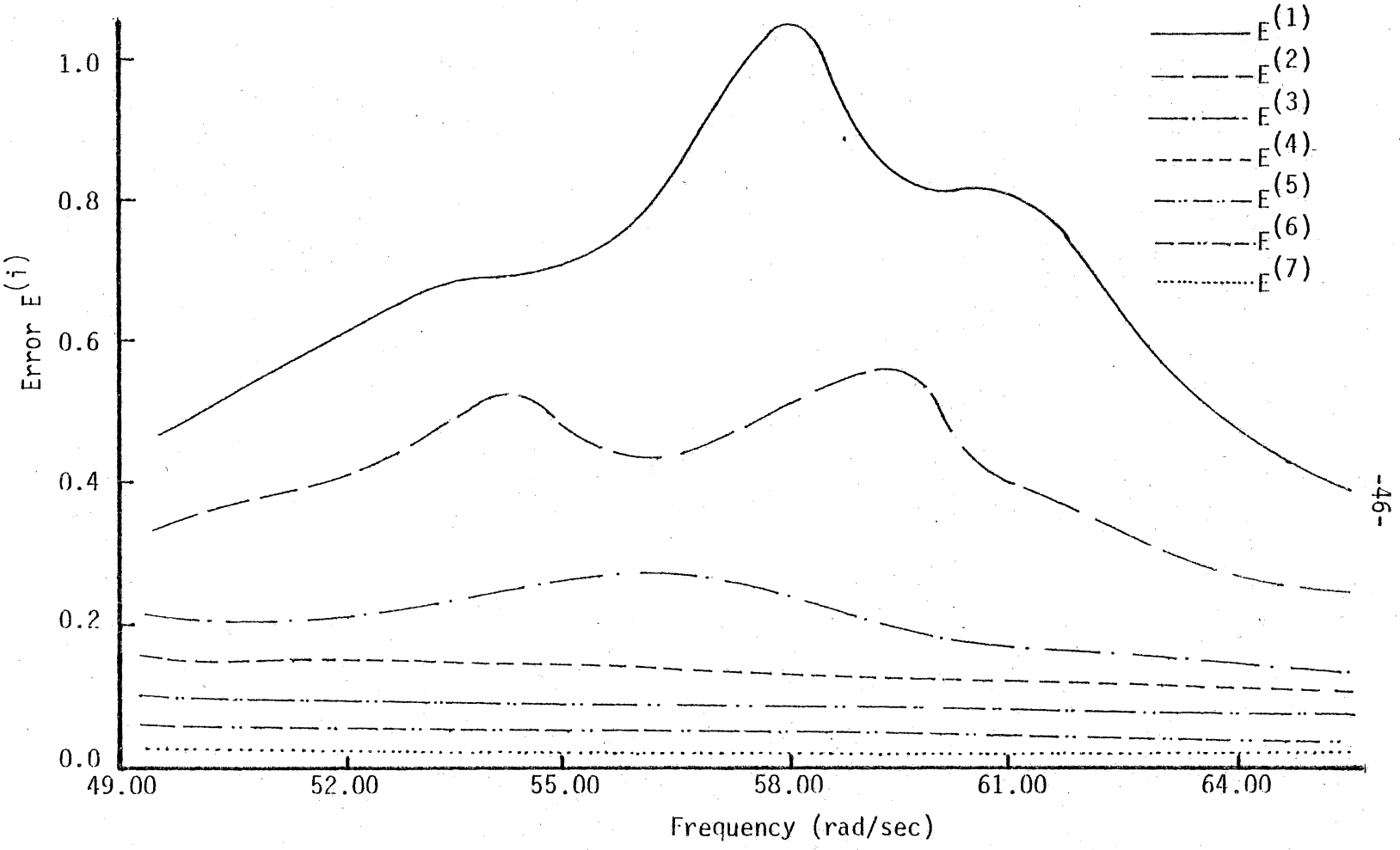

Figure 15.- Model 3, first region - Error plot with complete admittance matrix.

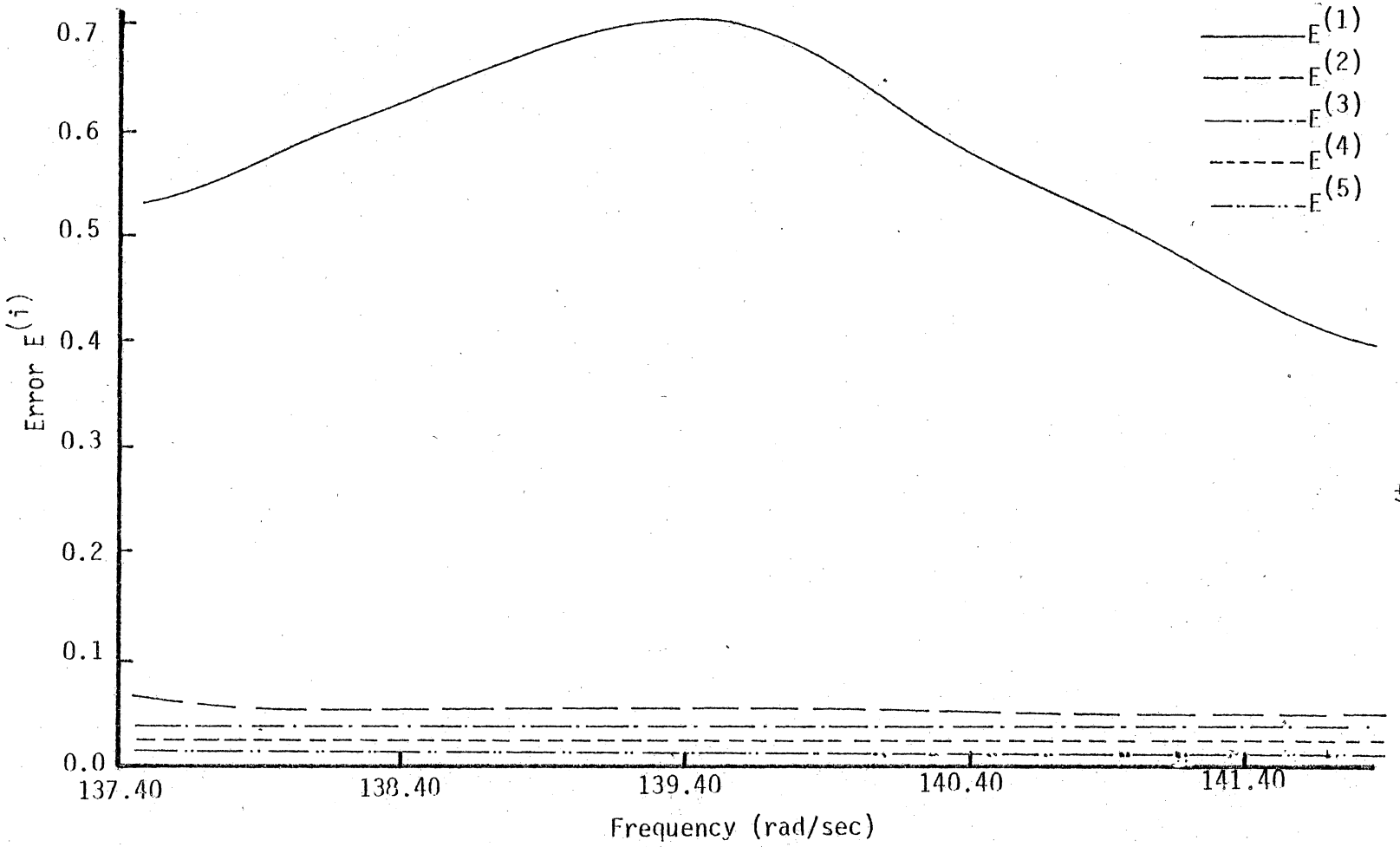

Figure 16.- Model 3, second region - Error plot with complete admittance matrix.

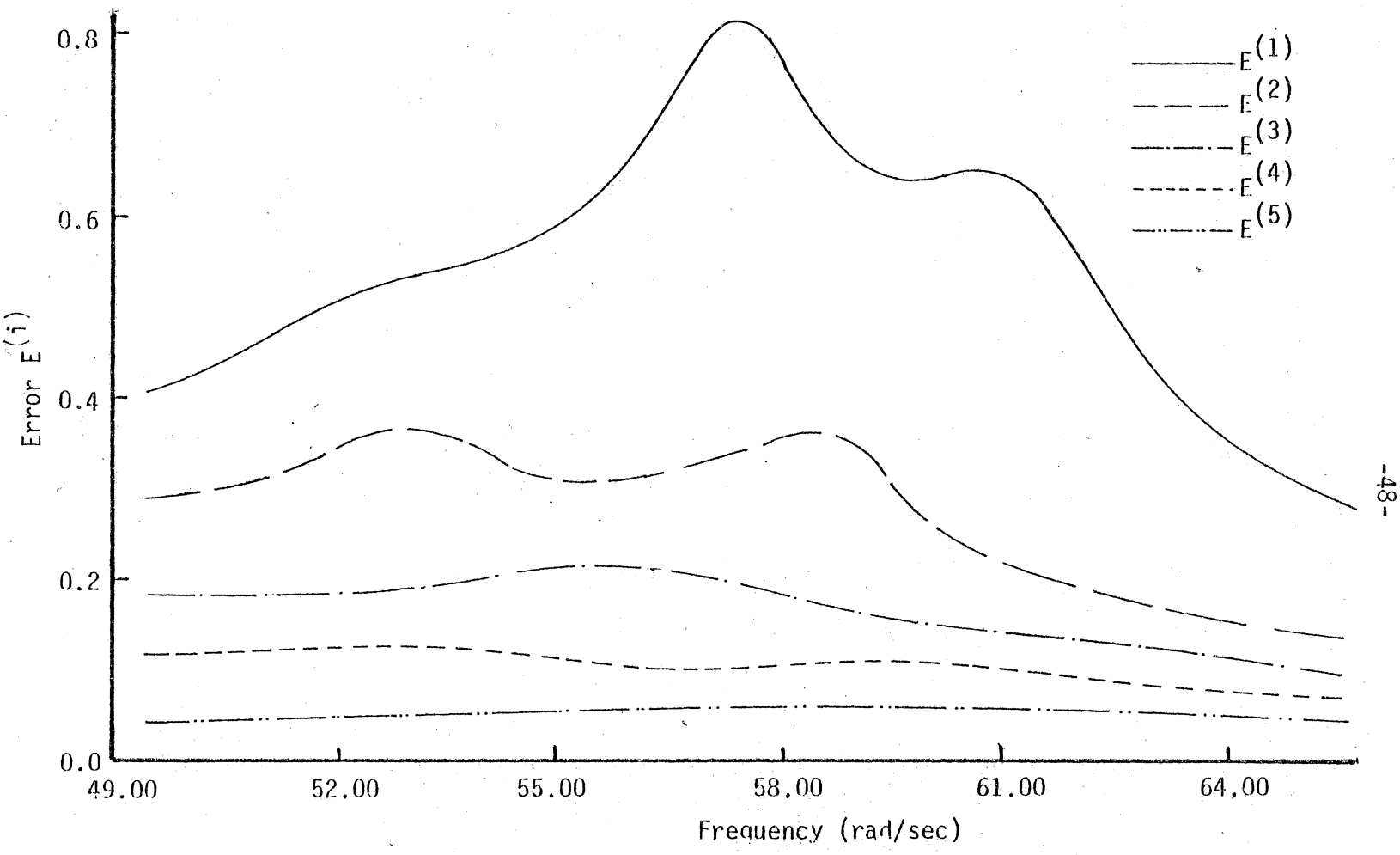

Figure 17.- Model 3, first region - Error plot with 8 sensors and 6 shakers. Sensors located at dofs 1, 2, 3, 5, 6, 7, 8 and 9, shakers located at dofs 1, 2, 3, 5, 6 and 9.

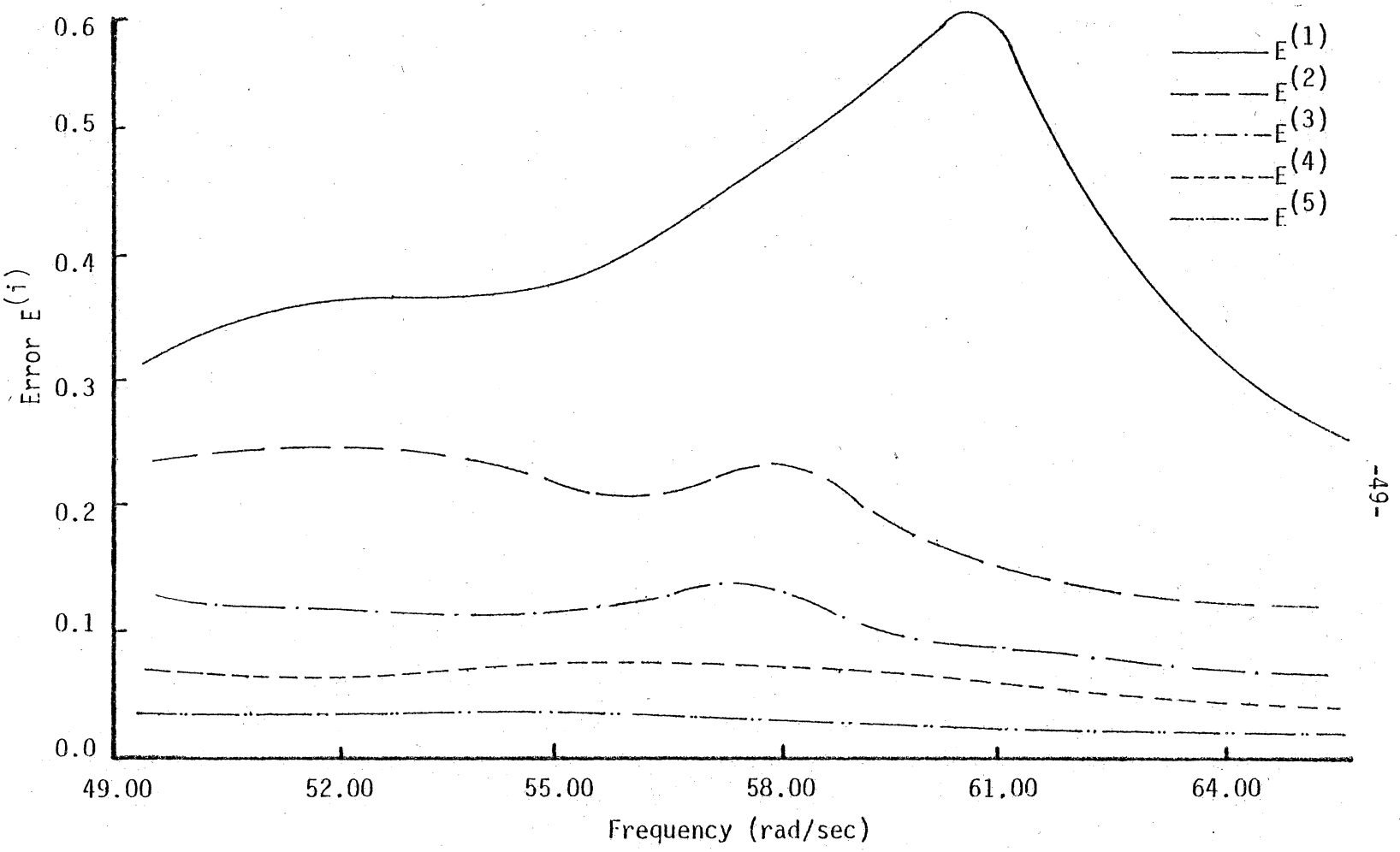

Figure 18.- Model 3,first region - Error plot with 7 sensors and 6 shakers. Sensors located at dofs 2, 3, 5, 6, 8, 9 and 10, shakers located at dofs 3, 4, 5, 6, 7 and 9.

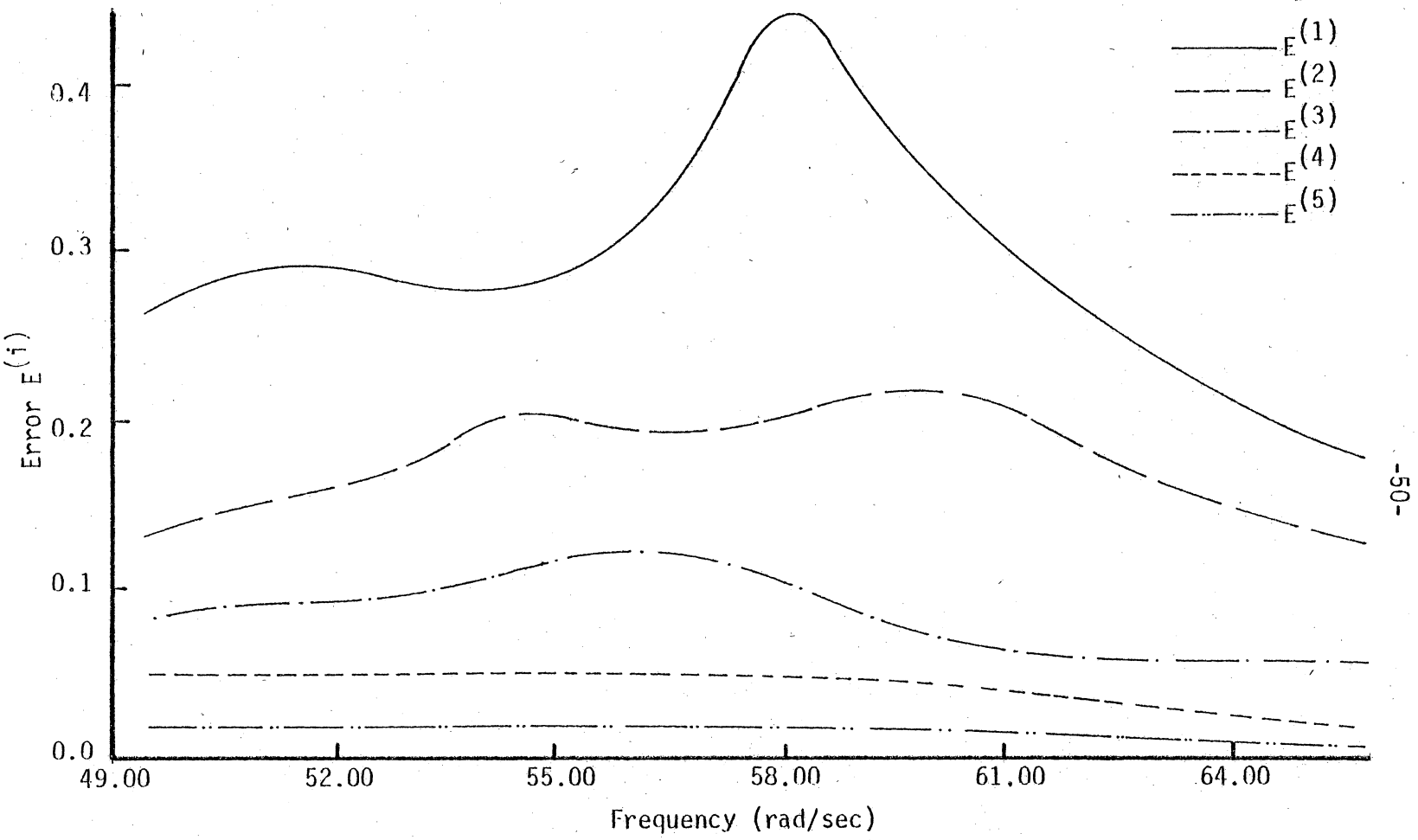

Figure 19.- Model 3, first region - Error plot with 6 sensors and 6 shakers. Sensors located at dofs 1, 3, 4, 6, 8 and 10, shakers located at dofs 2, 4, 5, 6, 8 and 9.

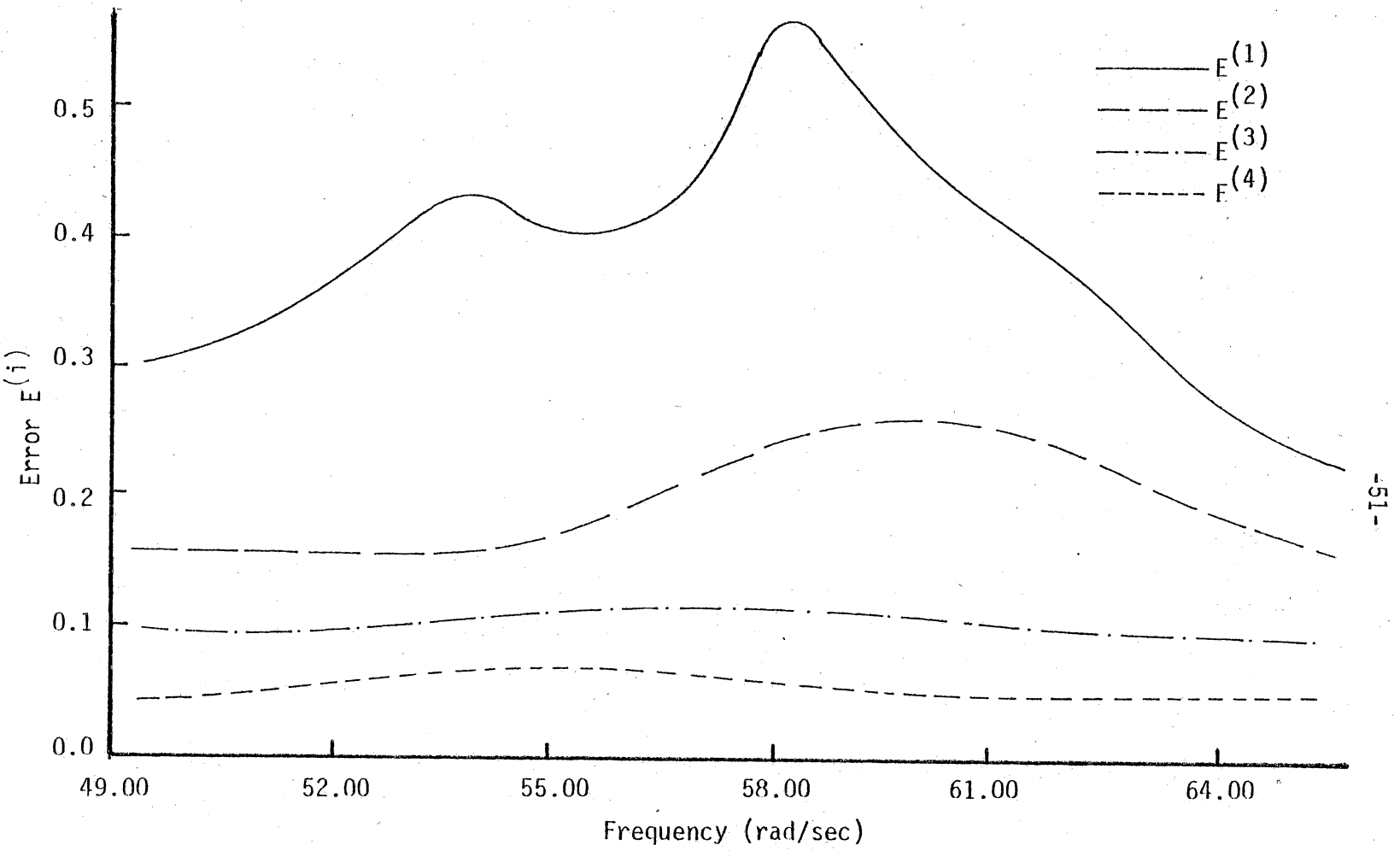

Figure 20.- Model 3, first region - Error plot with 10 sensors and 5 shakers. Sensors located at dofs 1, 2, 3, 4, 5, 6, 7, 8, 9 and 10, shakers located at dofs 2, 4, 6, 8 and 10.

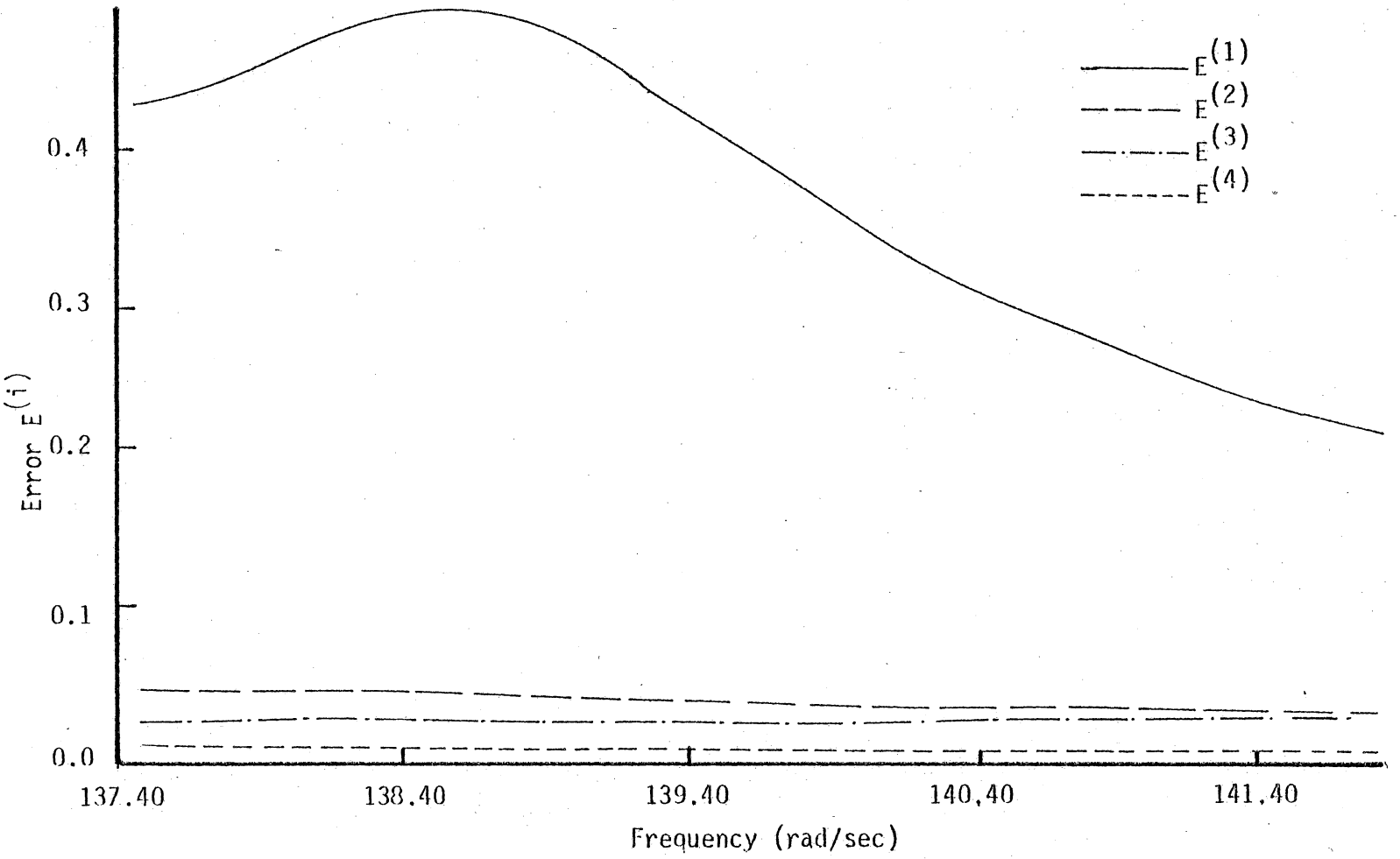

Figure 21.- Model 3, second region - Error plot with 8 sensors and 6 shakers. Sensors located at dofs 2, 3, 4, 6, 7, 8, 9 and 10, shakers located at dofs 2, 3, 5, 6, 8 and 9.

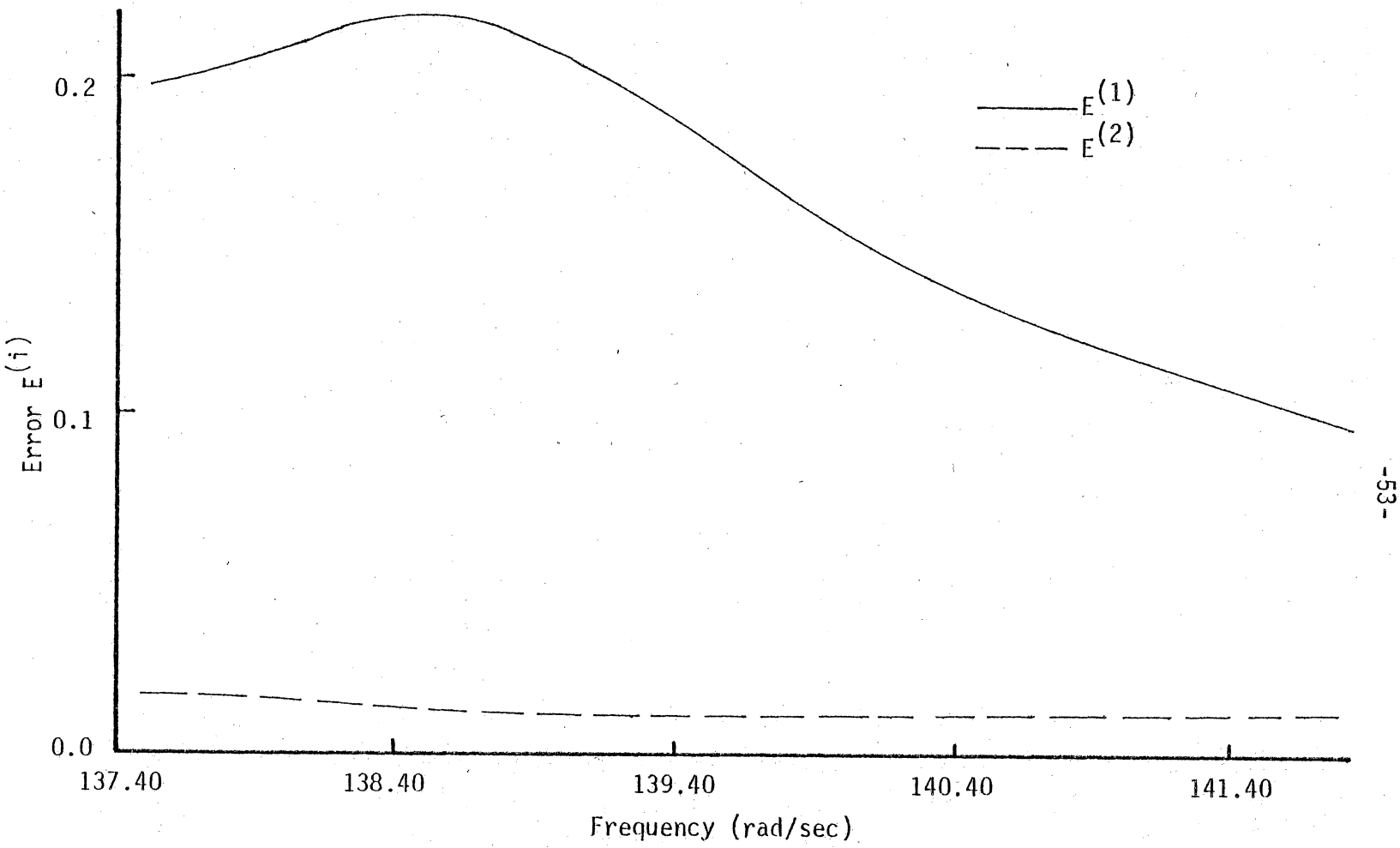

Figure 22.- Model 3, second region - Error plot with 5 sensors and 3 shakers. Sensors located at dofs 1, 3, 5, 7 and 9, shakers located at dofs 2, 5 and 8.

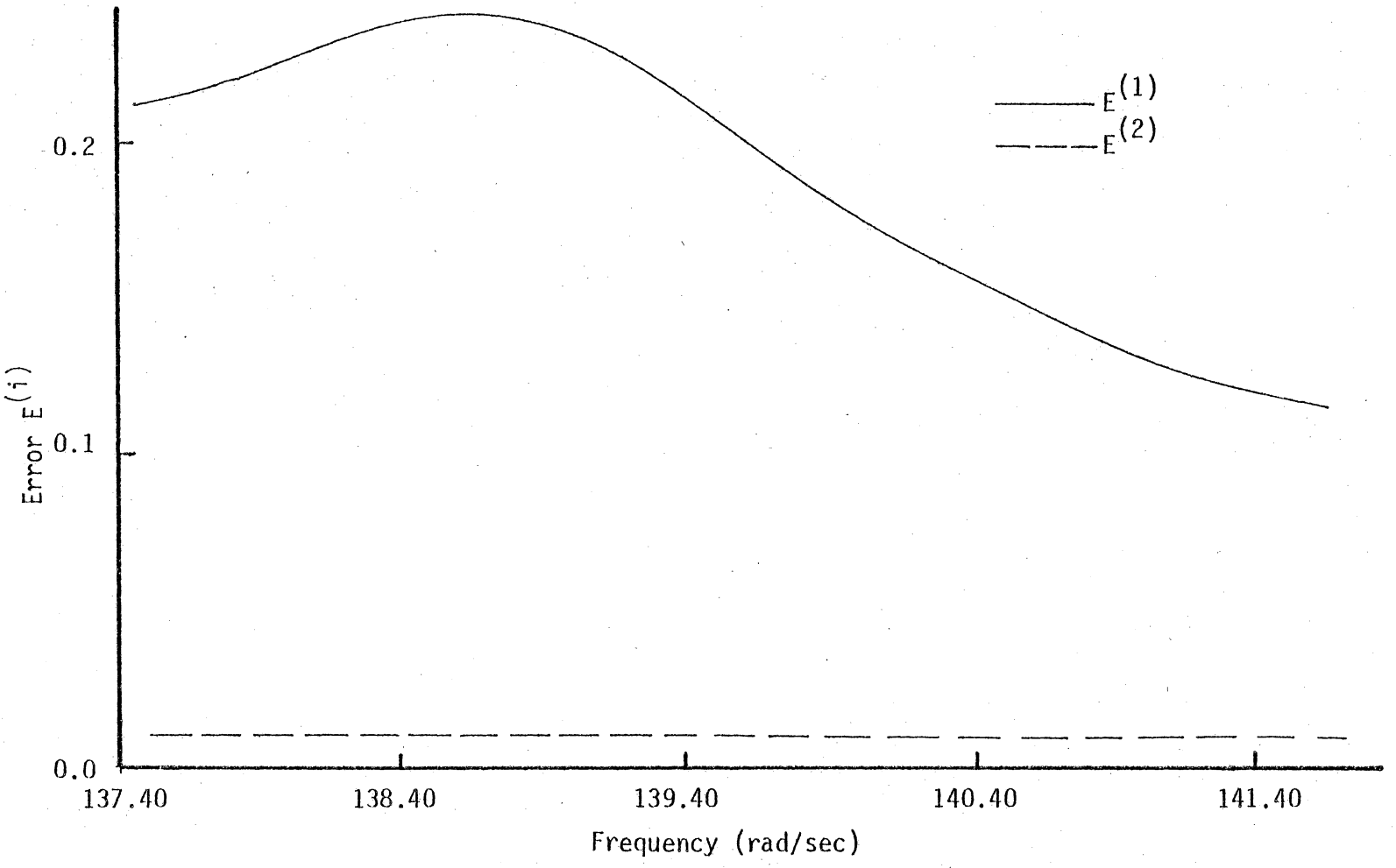

Figure 23.- Model 3, second region - Error plot with 5 sensors and 3 shakers. Sensors located at dofs 5, 6, 7, 8 and 9, shakers located at dofs 1, 2 and 3.

APPENDIX A

FLOW CHART DIAGRAM

FLOW CHART DIAGRAM

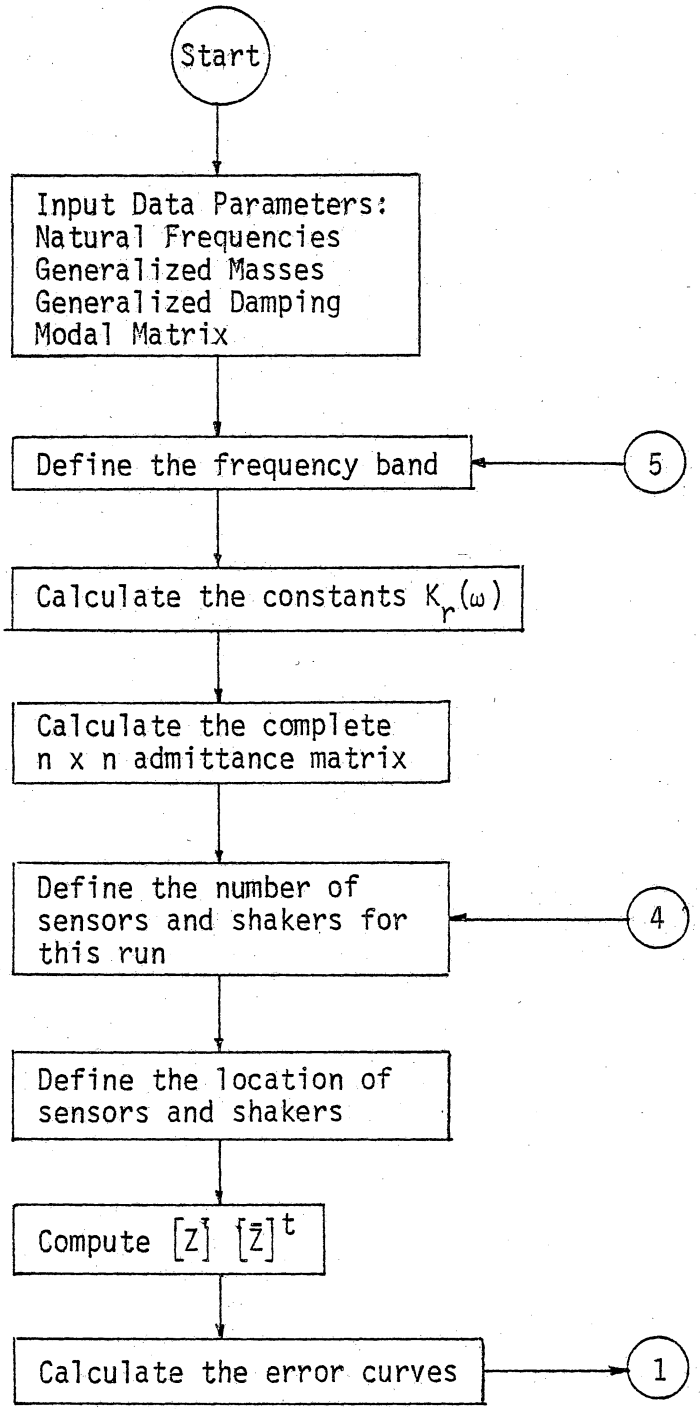

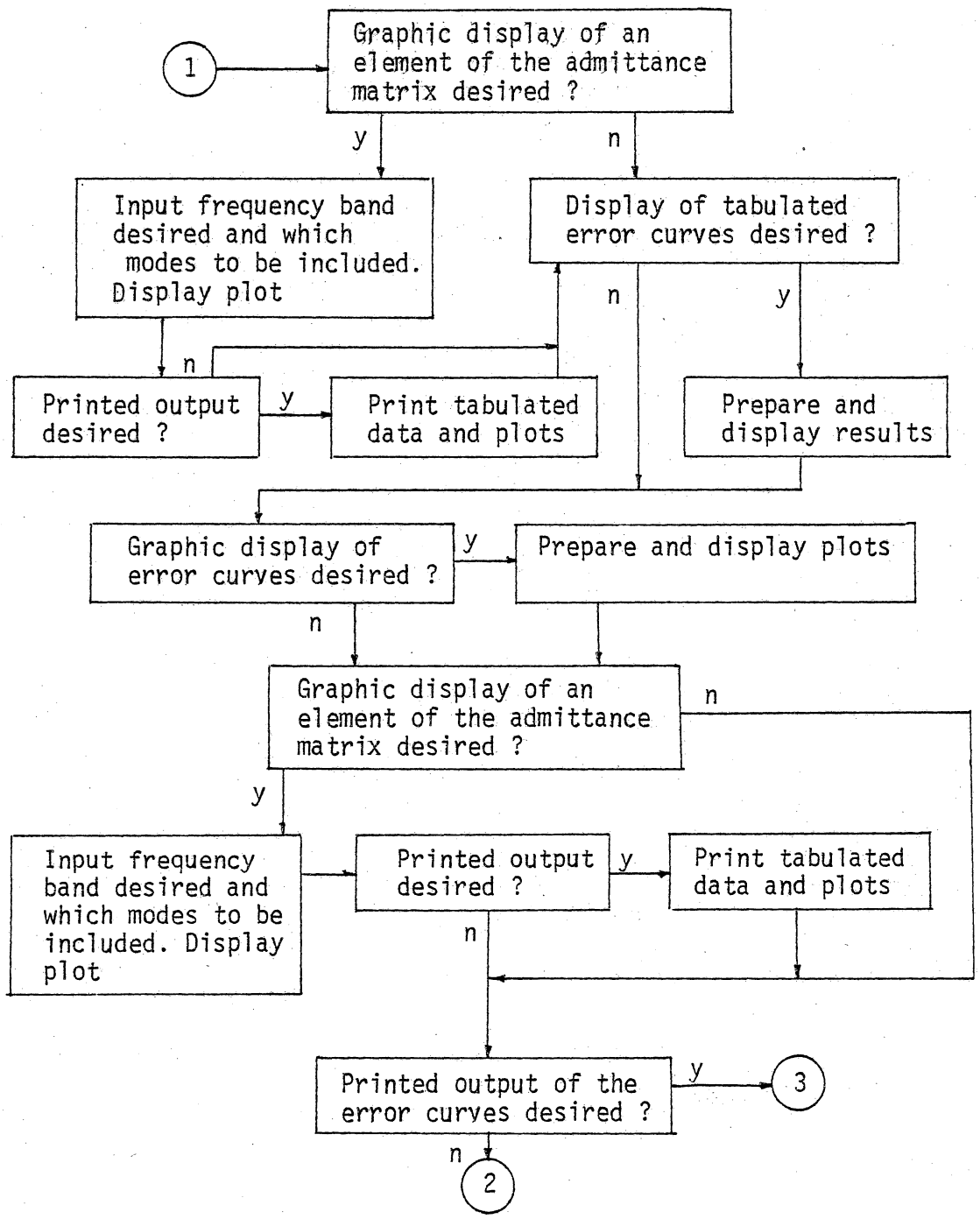
1
Graphic display of an element of the admittance matrix desired ?
y
n
Input frequency band desired and which modes to be included. Display plot
Display of tabulated error curves desired ?
n
y
n
Printed output desired ?
y
Print tabulated data and plots
Prepare and display results
Graphic display of error curves desired ?
y
Prepare and display plots
n
Graphic display of an element of the admittance matrix desired ?
n
y
Input frequency band desired and which modes to be included. Display plot
Printed output desired ?
y
Print tabulated data and plots
n
Printed output of the error curves desired ?
y
3
n
2

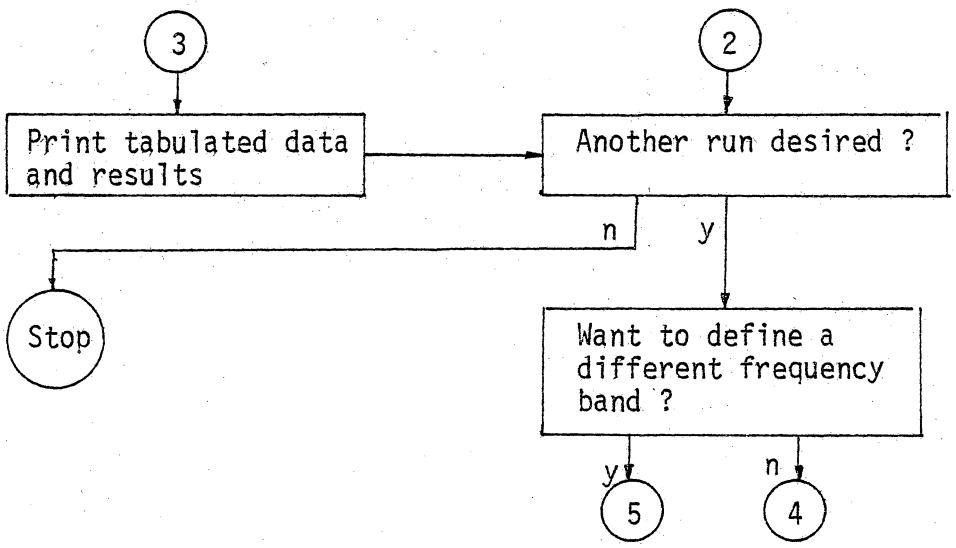
3
2
Print tabulated data and results
Another run desired ?
n
y
Stop
Want to define a different frequency band ?
y
n
5
4

APPENDIX B

DESIGN OF MATHEMATICAL MODELS

DESIGN OF MATHEMATICAL MODELS

The following discussion is included to help the reader understand the mathematical background in the design of Models 2 and 3. The parameters that had to be chosen were: natural frequencies, generalized masses, damping values and the modal matrix. They were chosen so as to simulate a certain number of dominant modes in a given frequency band. This can be best seen from a co-quad plot where the real versus the imaginary parts of the response are plotted.

If we consider the following n x n system with hysteretic non-coupling damping,

$$[m]\ddot{\underset{\sim}{x}} + \frac{1}{\omega}[kg]\dot{\underset{\sim}{x}} + [k]\underset{\sim}{x} = \underset{\sim}{F}\, e^{i\omega t}$$

it can be shown that, if one assumes the response to be of the form,

$$\underset{\sim}{x} = \underset{\sim}{X}\, e^{i\omega t}$$

using modal analysis we can solve for the forced response to obtain

$$\underset{\sim}{X} = [A]\,\underset{\sim}{F}$$

where the transfer function is

$$[A] = \sum_{r=1}^{n} \frac{\underset{\sim}{\phi}_r \, \underset{\sim}{\phi}_r^t}{M_r \omega_r^2 \{(1 - \beta_r^2) + i g_r\}}$$

or,

$$A_{ij} = \sum_{r=1}^{n} \frac{\phi_{ri} \, \phi_{rj}}{M_r \omega_r^2 \{(1 - \beta_r^2) + i g_r\}}$$

The contribution of the sth mode to A_{ij} is

$$A_{ij}^{(s)} = \frac{\phi_{si} \, \phi_{sj}}{M_s \omega_s^2 \left\{ \left(1 - \frac{\omega^2}{\omega_s^2}\right) + i g_s \right\}}$$

For ease of notation, denote

$$A_{ij}^{(s)} = \frac{C}{1 - \beta^2 + i g}$$

where $$C = \frac{\phi_{si} \, \phi_{sj}}{M_s \omega_s^2}$$

and $$\frac{A}{C} = \frac{(1 - \beta^2)}{(1 - \beta^2)^2 + g^2} + i \frac{-g}{(1 - \beta^2)^2 + g^2}$$

Using polar coordinates, a co-quad plot for a single mode is the exact circle shown in Figure B1, where the radius is a vector

$$r = - \frac{\phi_{si} \, \phi_{sj}}{M_s \omega_s^2 g_s} \sin\theta$$

and $$-\theta = \tan^{-1}\left\{\frac{g_s}{1 - \left(\frac{\omega}{\omega_s}\right)^2}\right\}$$

Notice that the frequency band from $\theta = -45^\circ$ to $\theta = -135^\circ$ is very narrow, namely from

$$\omega = \omega_s\sqrt{1 - g_s} \qquad (\text{at } \theta = -45^\circ)$$

$$\omega = \omega_s\sqrt{1 + g_s} \qquad (\text{at } \theta = -135^\circ)$$

If one more mode is present in this frequency band, then we would obtain a superposition of more than one radius vector, obtaining a plot such as that shown in Figure B2.

The parameters ω_s, M_s, g_s and ϕ_s in the design of Models 2 and 3 were chosen so as to obtain the type of interaction shown in Figure B2.

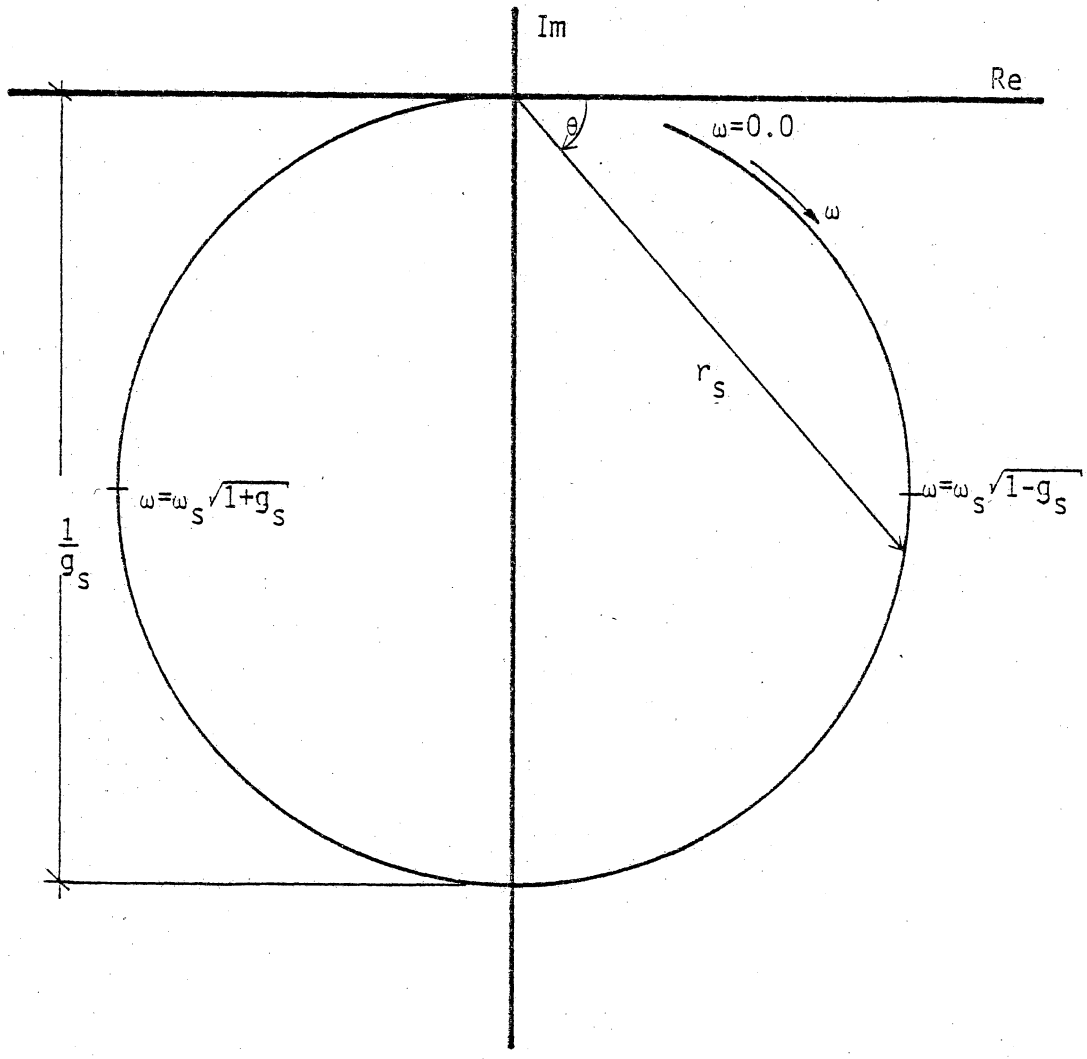

Figure B1.- Co-quad plot for one mode.

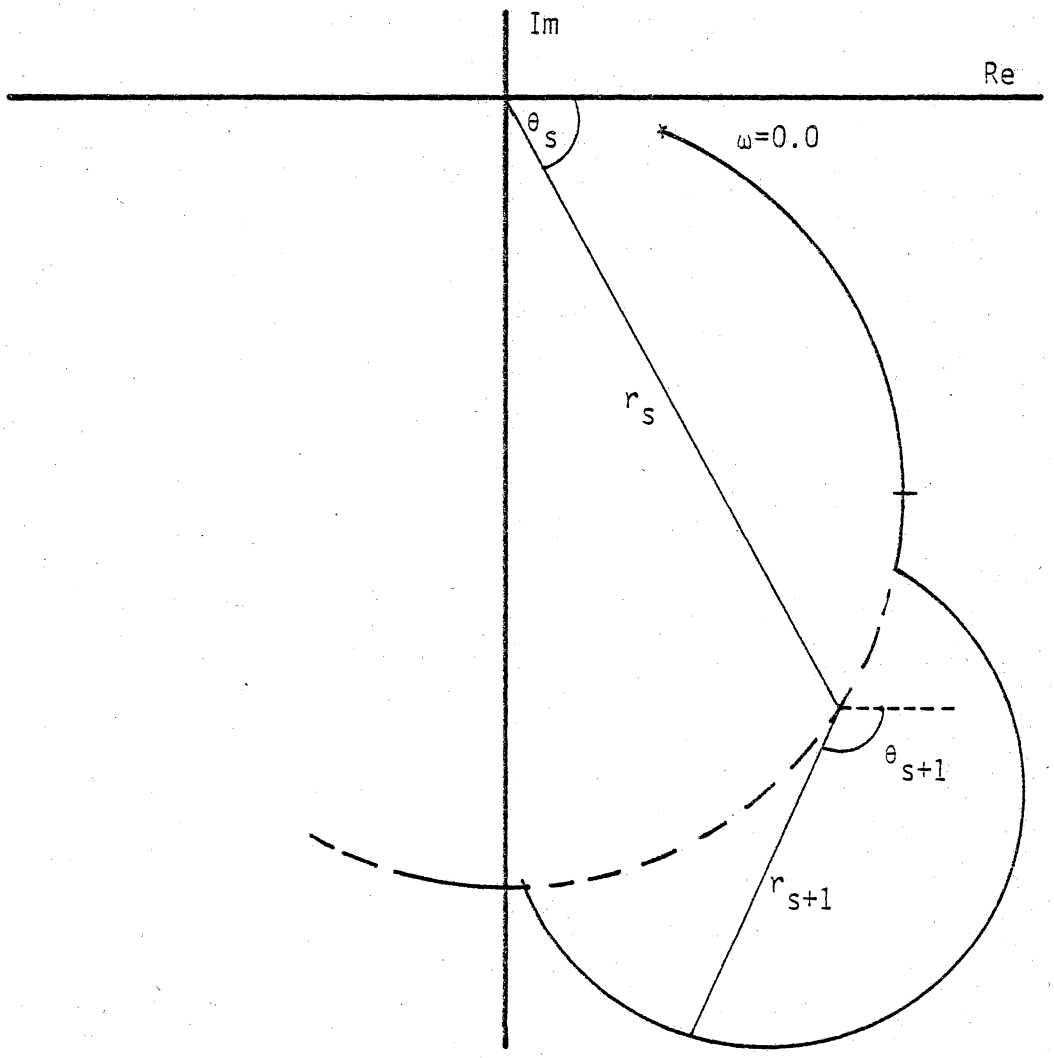

Figure B2.- Co-quad plot for two modes.

The vita has been removed from the scanned document

A METHOD FOR DETERMINING THE NUMBER OF DOMINANT MODES IN SINUSOIDAL STRUCTURAL RESPONSE

by

Ariel Franck

(ABSTRACT)

Modal analysis is a tool widely used to describe mathematically the vibratory behavior of structures. In modal analysis, the response of a structure at a given frequency of excitation is represented as the summation of the contributions of all the modes of vibration. Although continuous structures have an infinite number of modes, only a few of them are present to a significant degree in the response at any frequency of excitation. These modes are the dominant modes at the given frequency.

A vector fit method was developed to determine the number of dominant modes. This method uses only the transfer function matrix (or some part of it) as input, and it approximates each column vector of the matrix as a linear sum, using as a basis a set of orthogonal unit vectors. The errors resulting from these approximations, defined in a least squares sense, are the plotted versus frequency. The relative magnitudes of the error curves indicate the number of dominant modes in the frequency band in question.

The method was tested numerically on three models with known modal parameters. These models were designed to have regions of high modal density.

It was found that interpretation of the error curves required a certain amount of qualitative judgement based upon criteria other than simply the relative error magnitudes. With these criteria identified, it was concluded that the vector fit method reliably predicts the correct number of dominant modes provided only that a sufficiently large tranfer function matrix is employed. Specifically, both the number of rows and the number of columns must be greater than the number of dominant modes.